TRIBHUVAN UNIVERSITY
INSTITUTE OF ENGINEERING
PULCHOWK CAMPUS

Thesis No.: G011/075

Study of Stability of Slope Failure-The Case of Singati Landslide, Dolakha

by

Pawan Paudel

A THESIS

SUBMITTED TO THE DEPARTMENT OF CIVIL ENGINEERING

IN PARTIAL FULFILLMENT OF THE REQUIREMENTS FOR THE

DEGREE OF MASTERS OF SCIENCE IN GEOTECHNICAL ENGINEERING

DEPARTMENT OF CIVIL ENGINEERING

LALITPUR, NEPAL

April, 2023

COPYRIGHT

TRIBHUVAN UNIVERSITY

INSTITUTE OF ENGINEERING

PULCHOWK CAMPUS

DEPARTMENT OF CIVIL ENGINEERING

APPROVAL PAGE

The undersigned certify that they have read and recommended to the Institute of Engineering for acceptance, a thesis entitled **"Study of Stability of Slope Failure-The Case of Singati Landslide, Dolakha"** submitted by Pawan Paudel (075/MSGtE/011) in partial fulfilment of the requirements for the degree of Master of Science in Geotechnical Engineering.

_____

Supervisor: Dr. Mohan Prasad Acharya
Senior Geotechnical Engineer
NEA Engineering Company Limited

_____

Supervisor: Dr. Indra Prasad Acharya
Associate Professor
Institute of Engineering, Pulchowk Campus

_____

External Examiner: Bharat Bahadur Dhakal
Associate Professor
Institute of Engineering, Pulchowk Campus

_____

Program Coordinator: Dr. Santosh Kumar Yadav
M.Sc. Program in Geotechnical Engineering
Department of Civil Engineering,
Pulchowk Campus, Lalitpur, Nepal

April, 2023

ABSTRACT

This thesis presents a study of the stability of the slope failure. This study shows the real time interpretation of the slope using the field measured deformation in various season. The possible causes of instabilities are discussed by field visit judgments, field measurement data and results obtained. In this thesis, a method is presented to study the nature, amount and causes of deformation for the understanding of the slope failure and suggesting the mitigating measures. For this the pillars are installed in the study area and the measurements are taken relative to the pillar installation time in dry and wet seasons. The pore water pressure contribution in the deformation are analyzed. The results showed the increase in the deformation rate with increase in the water table of the slope.

The models are prepared using the cross section of the study slope and borehole log of core drilling in the study area. FEM software are used to back calculate the model material strength parameters using the field measurement deformation data.

The results from the FEM analysis are used to model in LEM and calculate the Factor of Safety value. Mitigation measures are suggested based on the results obtained from LEM. By decreasing the water table the Factor of Safety values increases and other protection measures along with drainage are suggested.

The Singati landslide slope is analysed for stability, vertical deformation, porewater pressure and mitigation measures.

Keywords: Slope, Slope Stability, Deformation, Water table, Factor of Safety, Mitigation

ACKNOWLEDGEMENTS

I wish to express my deepest and sincere appreciation to my supervisors Dr. Mohan Prasad Acharya and Associate Professor Dr. Indra Prasad Acharya for their guidance, encouragement and critical suggestion throughout the course of this study without whom, this research and thesis work couldn't achieve this state. I am highly indebted to them for their tireless patience during the thesis and for bearing with all the troubles and extending necessary help towards accomplishing this task. I highly appreciate their scholastic attitude and pragmatic thinking over thesis problems.

I am thankful to Department of Civil Engineering, Central Campus, and Staff of M.Sc. Program in Geotechnical Engineering for their support throughout my thesis work. My sincere thanks to Dr. Santosh Kumar Yadav and Dr. Bhim Kumar Dahal for their valuable guidance during my course work. I have deepest gratitude to NEA Engineering Company Limited for providing me necessary data and related information for conducting this research without whom this research would not be possible.

I would like to thank my friends Er. Biras Malla and Er. Ram Lamichane for their invaluable suggestions during my thesis.

In addition, I would like to thank my juniors Er. Prashant Giri and Er. Sunil tamang for helping in carrying out the survey works in the site.

Also, I must express my profound gratitude to my parents for their moral support and encouragement during my research period.

I would like to extend further thanks to all individuals for their direct and indirect help.

Pawan Paudel
075/MSGtE/011

TABLE OF CONTENTS

Contents

COPYRIGHT ..... **i**

APPROVAL PAGE ..... **ii**

ABSTRACT ..... **iii**

ACKNOWLEDGEMENTS ..... **iv**

LIST OF TABLES ..... **viii**

LIST OF FIGURES ..... **ix**

LIST OF ABBREVIATIONS AND SYMBOLS ..... **xi**

1. INTRODUCTION **1**

1.1. Introduction **1**

1.2. Background **2**

1.3. Objective **3**

1.3.1. General Objective **3**

1.3.2. Specific Objective **4**

1.4. Scope **4**

1.5. Methodology **4**

1.6. Content of this thesis **4**

2. LITERATURE REVIEW **6**

2.1. Slope Stability Analysis **6**

2.1.1. Limit Equilibrium Methods **6**

2.2. Back Analysis of Slope **7**

2.3. Back Analysis using Limit Equilibrium Method **9**

2.4 Back Analysis Using Finite Element Method **10**

2.5. Material Strength **10**

3. METHODOLOGY **12**

3.1. Site Visit Works....12

3.2. Desk Study and Literature Review....12

3.3. Installation of Pillar at Site for deformation data....12

3.4. Survey Works....14

3.5. Core Drilling Works....15

3.6. Estimating the Material Properties....16

3.7. Tools used for Modelling....16

3.7.1. Roc Science Phase 2.0....16

3.7.1.1 Steps Requirements for solution of the problem in Roc science Phase 2 software....17

3.7.2. Geo studio 2018....17

3.7.2.1 Step requirements for problem solving in Geo studio 2018 software....18

3.8. Use of Back Analyzed In-situ parameters....19

3.9. Solution to the Slope Stability Problems....19

4. Field Measurement....20

4.1 Field Measurement data during Installation of Pillars....21

4.2 Field Measurement Data during Chaitra Month....22

4.6 Field Measurement Data during Shrawan Month....22

4.3 Observed Vertical deformation by plotting Z data in various seasons....23

4.4 Observed Deformation in X direction in study period....26

4.5 Observed Deformation in Y direction in study period....26

4.7 Variation of X in Chaitra to Shrawan Month....27

4.8 Variation of Y in Chaitra to Shrawan Month....27

4.9 Observed deformation in Z direction in dry period....28

4.10 Observed deformation in Z direction in wet period....28

4.11 Discussion on the field measurement data....29

5. Numerical Modelling and Results....30

5.1 Model in FEM using borehole log 31

5.2 Vertical Deformation after 1m rise in water table.....32

5.3 Vertical Deformation after 3m rise in water table.....33

5.4 Vertical Deformation after 4m rise in water table.....34

5.5 Vertical Deformation after 5m rise in water table.....35

5.6 Vertical Deformation after 6m rise in water table.....36

5.7 Vertical Deformation after 7m rise in water table.....37

5.8 Vertical Deformation after 8m rise in water table.....38

5.9 Horizontal deformation after 8m rise in water table.....39

5.10 Total deformation after 8m rise in water table 40

5.11 Vertical Deformation after 9m rise in water table.....41

5.12 Vertical Deformation after 10m rise in water table.....42

5.13 Model in LEM for FOS determination 43

5.14 FOS at 8m rise in water table 44

5.15 FOS at 7m rise in water table 46

5.16 FOS at 6m rise in water table 47

5.17 FOS at 3m rise in water table 48

6. Discussion 50

7. Conclusion 55

8. References.....57

LIST OF TABLES

Table 3. 1: Data range considered for parameter fixation 20

Table 4. 1: Field measurement data of Falgun Month 20

Table 4. 2: Field measurement data of Chaitra month.....21

Table 4. 3: Field measurement data of Shrawan month 21

Table 4. 4: Observed deformation data in X direction in Falgun to Shrawan 25

Table 4. 5: Observed deformation data in Y direction in Falgun to Shrawan 25

Table 4. 6: Observed deformation data in X direction in Chaitra to Shrawan 26

Table 4. 7: Observed deformation data in Y direction in Chaitra to Shrawan 26

Table 4. 8: Observed deformation data in X direction in Falgun to Shrawan 27

Table 4. 9: Observed deformation data in X direction in Falgun to Shrawan 27

Table 6. 1: Model parameters obtained from back analysis in FEM..... 49

Table 6. 2: Factor of Safety values obtained from LEM for variation in water table..... 50

LIST OF FIGURES

Figure 1. 1: Location of Singati Landslide 1

Figure 1. 2: Under Construction building damaged by landslide 2

Figure 1.3: Soil Materials as seen on surface in landslide zone 3

Figure 2. 5: Graphical representation of Coulomb Shear Strength equation 10

Figure 2. 6: Mohr- Coulomb failure envelop 11

Figure 3. 1: Location of Instrumented Pillars ……13

Figure 3. 2: Pillar number 10 installed at the study area 14

Figure 3. 3: Cross section of the studied slope 14

Figure 3. 4: Recording the data of Pillar number 7 using total station at the study area 15

Figure 3. 5: Plot of Cross section with different material boundary and GWT 16

Figure 3. 6: Mesh set up and restrain in X and Y directions 17

Figure 4.1: Location of Installed Pillars in the study area..... .19

Figure 4. 2: Plot of Z value in Pillar 1 and Pillar 2 in various months 22

Figure 4. 3: Plot of Z value in Pillar 3 and Pillar 4 in various months 22

Figure 4. 4: Plot of Z value in Pillar 5 and Pillar 6 in various months 23

Figure 4. 5: Plot of Z value in Pillar 7 and Pillar 8 in various months 23

Figure 4. 6: Plot of Z value in Pillar 9 and Pillar 11 in various months 23

Figure 4. 7: Plot of Z value in Pillar 12 and Pillar 13 in various months 24

Figure 4. 8: Plot of Z value in Pillar 10 in various months..... 24

Figure 4. 9: Vertical Deformation in various seasons 28

Figure 5. 1: Model in FEM for deformation back analysis 30

Figure 5. 2: Result for vertical deformation after 1m rise in water table..... 31

Figure 5. 3: Result for vertical deformation after 3m rise in water table..... 32

Figure 5. 4: Result for vertical deformation after 4m rise in water table..... 33

Figure 5. 5: Result for vertical deformation after 5m rise in water table 34

Figure 5. 6: Result for vertical deformation after 6m rise in water table..... 35

Figure 5. 7: Result for vertical deformation after 7m rise in water table..... 36

Figure 5. 8: Result for vertical deformation after 8m rise in water table..... 37

Figure 5. 9: Result for horizontal deformation after 8m rise in water table 38

Figure 5. 10: Result for total deformation after 8m rise in water table 39

Figure 5. 11: Result for vertical deformation after 9m rise in water table 40

Figure 5. 12: Result for vertical deformation after 10m rise in water table 41

Figure 5. 13: Model in LEM..... 42

Figure 5. 14: Model in LEM for calculating FOS of back analyzed parameters..... 43

Figure 5. 15: FOS calculation at 8m water table from original water table 44

Figure 5. 16: FOS calculation at 7m water table from original water table 45

Figure 5. 17: FOS calculation at 6m water table from original water table 46

Figure 5. 18: FOS calculation at 3m water table from original water table 47

Figure 5. 19: Expanded view of FOS calculation at 3m water table from original water table……..49

Figure 6. 1: FOS calculation at original water table..... 52

Figure 6. 2: FOS calculation after strength regain consideration 53

Figure 6. 3: Recommended protection measures..... 54

LIST OF ABBREVIATIONS AND SYMBOLS

LEM	Limit Equilibrium Method
FEM	Finite Element Method
BH1	Bore Hole 1
BH2	Bore Hole 2
FOS	Factor of Safety
X2	Cross section 2
X	Easting
Y	Northing
Z	Elevation
kPa	Kilo Pascal
kN	Kilo Newton
c'	Cohesion
Φ'	Angle of friction

1. INTRODUCTION

1.1. Introduction

Nepal witnesses' large number of slope instability resulting huge loss of properties, lives. Stability of slope is most challenging as well as most vital in developing country like Nepal for the safety of human lives, properties and infrastructures of the area. Slope stability analysis is performed to access the safety and economic design of the slopes that may be cut slopes, embankments or the slope in natural existing state.

Landslide is observed at the slope in the Singati Bazar of Dolakha district. The barrier in the river pushed by the slide is visible. There is the settlement in the area of the slide. The debris from the slide have disturbed the buildings which are in its path. This slope instability may result huge destruction of properties, human lives and infrastructures nearby. The landslide phenomenon is also observed in the reconnaissance survey of the area (the transmission tower had been distorted). The soil type observed are (Boulder mixed soil, silty soil, and pebble-boulder of gray fine to coarse grained sand with flakes of schist as Figure 1.3).

Figure 1. 1: Location of Singati Landslide(Source: Google Earth)

Figure 1. 2: Under Construction building damaged by landslide.

This study gives the clear insight of the stability analysis of the slopes failure using different methods of analysis by numerical modelling and field verifications of the specified Singati landslide. The rate of deformation is analyzed for different seasons. The cause of the slope instability is analyzed. LEM software is used to analyze the mitigation model of the determined slope instability causes. The model incorporates the methodology for suggesting the suitable mitigating measures to make the slope stable. The results presented validated the methodology presented.

1.2.Background

Slope instability have been the major cause for the destructions in the hilly and mountainous regions of Nepal resulting huge losses of human lives, properties, infrastructures yearly. Although the slow moving landslides rarely cause huge damage but it can cause huge destructions if triggering factors trigger the rapid movements.

Landslide is observed at the slope in the Singati Bazar of Dolakha district. The continuous movement was observed from the analysis of Google images even before the constructions of road in the region. After the excavations for the road construction, the proper drainage facilities was not provided. The water flow from the agricultural land through the road in to the slopes might be the triggering factor for the movement. The

building which is under construction is damaged as seen in Figure 1.2. The infrastructures like road, bridge over Singati River are subjected to risk. The transmission tower which was constructed on the landslide zone by damaged by this landslide phenomenon.

Figure 1.3 Soil Materials as seen on surface in landslide zone

1.3. Objective

The objectives of this study are divided in to two categories basically general and specific objectives.

1.3.1. General Objective

The general objectives of this study are listed as follows:

- Study the nature, amount and cause of deformation for the understanding of slope failure.
- Analyze the slope for the assessment of Stability.
- Recommendation of stabilizing measures.

1.3.2. Specific Objective

- To analyze the slope stability of the study area from the Numerical modelling with verification from deformation measurement to determine and evaluate the cause of slope movement.
- To analyze the performance of mitigation measures such that it can further verify the major triggering factor of slope movement.

1.4. Scope

The stability analysis of instability zone of about 0.11 km^2 is performed. Boreholes data at two locations and profile survey along the study area data is collected, analyzed.

1.5. Methodology

This thesis or this study presents the ways to analyze the slope instability of the any region. The method is presented to analyze the causes and mitigations measures for the instability of the slope. The methodology chapter presents the analysis procedure for analyzing the instability cause and mitigation modelling of the study area. Profile survey of the region is done to generate the slope model and to determine slope angle. Traverse survey of the study area and instrumentation to determine the deformation at that location is carried out. Bore hole drilling is conducted in two locations for the soil samples collection and to generate the soil profile and to make soil depth models, Soil profile, GWT Location, Index and engineering properties of soils along the alignment. The material modelling of slope material is performed. The deformation data obtained from instrumentations and the judgments during the site visit are analyzed to determine the causes of the landslide. These deformation data are used to back calculate the soil parameters. Further, LEM software is used for mitigation modelling and verification of proposed mitigation of the instability area or the study area.

1.6. Content of this thesis

This thesis is made up of seven chapters. The chapter first is introduction and it introduces overall thesis works. The contents, the methods followed for this study, the intended results are presented lightly in the introduction chapter. Chapter two is literature review which elaborated the review of the literatures, papers, documents, previously completed thesis, journal papers, and various publications regarding the stability analysis, causes and mitigation measures for the landslides observed in the soil

type found in this study. In chapter three the method adopted for meeting the objectives of this thesis is presented. Different parameters required for analysis are developed for back analysis using deformation data and FOS determination and mitigation of the slope instability. In chapter four Field Measurements are presented and discussed. In chapter five, Numerical modelling of the slope are prepared and analysis are discussed with the obtained results. In chapter six and seven Discussion of the results and Conclusion of study is discussed.

2. LITERATURE REVIEW

2.1. Slope Stability Analysis

Slopes may be artificial or natural. In either case, forces exist which tend to cause the soil to move from the high points to the low points. There is the inherent tendency in the slopes to achieve the stable positions. If there is any tendency for slope to move, it can be considered as instability. If the actual movement in the slope occurs, it is a slope failure. Slope failure is a common phenomenon around the world. Slope failure has been the common problem in context of Nepal also causing the huge toil on human life and damage of properties. Prior to, during, and after the building of any structure, the slopes must be properly evaluated. The development of the 21st century has brought about wonders of geotechnical engineering, as well as human-made constructions like roadways, railroad embankments, hydraulically produced dams, earth dams, etc. Geotechnical engineering's study of the stability of both naturally occurring and artificially created slopes is crucial in this regard.

The factor of safety of artificial and natural slopes can be calculated in a variety of ways, such as limit equilibrium, finite element methods, finite difference methods, discrete element methods, soft computing, etc. The limit equilibrium approach is a common technique used in these methods, a technique for analyzing slope stability in which the stability of the slope is predicted from a single value of the factor of safety. Later, several researchers created finite element methods as a potent way for deriving solutions to slope stability issues. Nevertheless, reliability and risk are tied to the issue of slope stability. So, it is impossible to take safety precautions against slope failure by relying solely on one component of safety. The reliability Index for a slope or other measure is calculated in order to analyze the reliability of slopes. (Sami Ullaha , Muhib Ullah Khanb and Gohar Rehmana).

The choice of analysis method will depend on the nature of the problem, the quality and type of input data which is available, the type of analysis results which are required and the level of expertise and preference of the researcher.

2.1.1. Limit Equilibrium Methods

The Limit Equilibrium Method, generally known as LEM, is one of the oldest techniques created to analyze the stability of slope. Calculations of applied stress and mobilized strength in the slope of a test slide surface are necessary. These two provided quantities

are used in this instance to measure safety factor. Trial failure surfaces in this regard calculate the least and most critical value. There are numerous additional methods in this class. The key distinction between the many methods of limit equilibrium, such as circular, planar, logarithmic, etc., is provided by the assumptions relating to the geometry of the sliding surface. Whereas moment or force equilibrium, or sometimes both, are based on the same assumptions as the equilibrium equation. Sometimes the third dimension, which runs perpendicular to the cross-sectional plane and affects the slope's outcome, is taken into account (Albataineh, 2006). For the analysis of slope stability, Slice methods are typically utilized in limit equilibrium approaches. There are various LEMs which of some main are listed below and discussed:

- The Ordinary Method of Slices
- Bishop's Methods
- Modified Bishop Methods
- Janbu's Method
- Morgenstern- Price Method
- Spencer's Method
- Corps Of Engineers Method
- Sharma Method
- Lowe-Karafiath Method

2.2. Back Analysis of Slope

Two independent methods are often used to execute the slope stability study: forward analysis and back analysis. When a slope fails, back analysis is performed to ascertain the condition of the slope at that point, including the mobilized strength and the pore-water pressure. Forward analysis is used to evaluate whether a slope is operating safely as it was meant to.

The slope stability parameters can be back analyzed using either a deterministic or

probabilistic approach (Duncan et al., 2005). The deterministic approach looks for a single set of parameters that might be to blame for the failure. When several sets of slope stability parameters need to be back-analyzed simultaneously under uncertainty, back analysis is carried out in a probabilistic manner (Zhang et al, 2010). A probability distribution of the results is constructed, from which the failure probability is computed, and the uncertain parameters are modelled as random variables. By including the slope failure data, the distribution can be further enhanced.

Back and inverse analyses are generally well known as the computational techniques which can provide required information about unknown parameters controlling an investigated system or phenomenon using data generated as its output behavior.(Piotr SROKOSZ, 2008)

Measuring soil strengths by back analysis is popular, particularly in connection with landslide repairs because it eliminates several issues with laboratory testing.

Back analysis is a useful technique for including critical elements that may not be adequately captured in laboratory samples, such as the soil's structural makeup, its lack of homogeneity, the impact of fissures on soil shear strength, and the implications of pre-existing shear planes within the soil mass. In order to estimate the soil shear strength that was mobilized for the failure to have occurred in accordance with the two-dimensional limit equilibrium model, for example, Spencer's (1967) method, adopted for analysis, a back analysis assumes the original slope geometry and a factor of safety equal to unity. The soil shear strength that was mobilized is obtained from this back calculation. The shear strength metrics, cohesion, and internal friction angle of failed materials as evaluated by laboratory and in-situ experiments may be uncertain because of the representative sample of the materials involved in the possible failure surface and simulation of field condition existing in the slope. The mobilized parameters can be estimated in-situ more accurately and consistently with the use of back analysis approach. (Wilson H. Tang, Timothy D. Stark and Mauricio Angulo).

The factor of safety is equal to unity, which is the only piece of information a slope failure offers. In order to produce a factor of safety equal to unity, the shear resistance might be changed.

The shear resistance is usually governed by the combination of c' and ϕ'. If the position of the failure surface is controlled by the location of strong or weak layers within the

slope, the shear resistance can be calculated because the location of the failure surface is known and not a function of the combination of c' and ϕ'. If the required shear resistance and the corresponding effective stress are known, a combination of c' and ϕ' can be selected to represent the required shear resistance on the failure surface. (Wilson H. Tang, Timothy D. Stark and Mauricio Angulo).

Back Analysis of slope is reliable when the model and all assumptions are reasonable and accurate representations of the real system. (Rick Deschamps and Greg Yankey). Back analysis of the slope failure is often performed to improve one's knowledge on parameters of a slope stability analysis model (J. Zhang, Wilson H. Tang, and L.M. Zhang, Geotechnical paper 2010) i.e., the material properties obtained from laboratory result or engineering judgment can only be an initializing value to the slope stability analysis problem and Back analysis is carried out to improve the results.

It should be noted that a back analysis does not always indicate that failure has happened. Back analysis can also refer to the process of identifying the necessary material characteristics or supporting force to achieve a particular level of safety or reliability. (Slide 6.0 manual)

2.3. Back Analysis using Limit Equilibrium Method

According to Duncan et al. (2005), there are two approaches for back analyzing the slope stability parameters: deterministic and probabilistic. The deterministic approach seeks to identify a single set of parameters that could result in failure. When it is necessary to simultaneously back-analyze numerous sets of slope stability parameters under uncertainty, back analysis is carried out in a probabilistic manner (Zhang et al, 2010). In order to calculate the chance of failure, a probability distribution of the results is created based on the unknown parameters' modeling as random variables. By including the slope failure information, the distribution can be made even better.

It is assumed that all the variables are known in the deterministic analysis which is far from reality due to the uncertainty of the available field data.

Statistical distributions are applied to the input parameters in the probabilistic analysis to account for the uncertainty in their values (Jagriti Mandal, Sruti Narwal, and S. S. Gupte).

Geostudio software can be used to conduct LEM. The sampling technique utilized for the probabilistic analysis is Monte Carlo simulation. To identify a single critical failure surface, the deterministic analysis is initially performed using the mean of all the input

parameters.

Once the critical failure surface's position is identified, a probabilistic analysis of the surface is carried out utilizing generated samples of the chosen random variables.

2.4 Back Analysis Using Finite Element Method

Phase 2.0 Software can be used for the FEM.

2.5. Material Strength

The most common way of describing the shear strength of geotechnical materials is by Coulomb's equation which is:

$\tau = c + \sigma_n \tan\phi$ where,

τ = shear strength (i.e., shear at failure),

c = cohesion,

σ_n= normal stress on shear plane, and

ϕ= angle of internal friction (phi).

A shear strength versus normal stress plot is represented by this equation by a straight line. The cohesion (c) is the line's intercept on the shear strength axis, and the angle of internal friction (ϕ) is its slope.

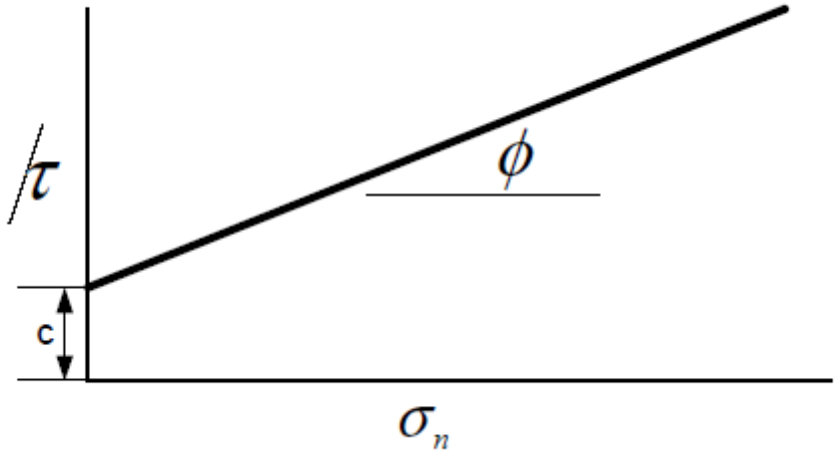

Figure 2. 5: Graphical representation of Coulomb Shear Strength equation

The failure envelope is frequently determined via triaxial testing, and the findings are expressed in terms of half-Mohr circles, as illustrated in Figure 2.6. Hence, the failure envelope is also known as the Mohr-Coulomb failure envelope.

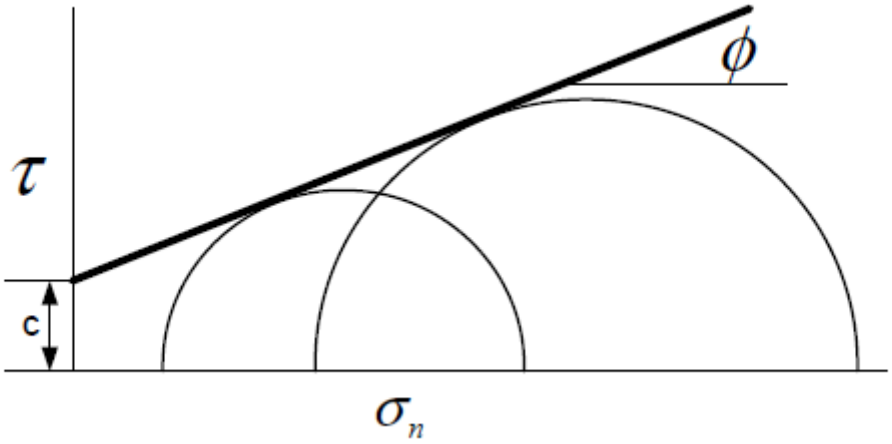

Figure 2. 6: Mohr- Coulomb failure envelop

The strength parameters c and ϕ can be total strength parameters or effective strength parameters. Effective strength parameters provide the most realistic solution, especially in regards to where the critical slip surface is located, from the perspective of slope stability analysis. When you apply effective strength parameters, the estimated critical slip surface position is the most realistic. When doing a slope stability study using solely undrained strengths, the location of the slip surface with the lowest factor of safety is not always close to the location of the actual slip surface in the event that the slope fails. For an assumed homogenous section, this is especially true.

3. METHODOLOGY

3.1. Site Visit Works

Site visit has been made for the reconnaissance of the study area and general geology, topography of the area was done in the first site visit. Area for the instrumentation of the pillars for the deformation data was specified.

In the second site visit, Survey of the study area was carried out. The measurement of the co-ordinates of the instrumented pillars were taken in the month of Falgun.

Third site visit was made to record the deformation data in the month of Chaitra.

The deformation data was recorded in the month of Shrawan.

3.2. Desk Study and Literature Review

The necessary books, literature, research paper is collected and studied. The LEM and FEM software is collected. The borehole log of the core drilling investigation is collected. It contains cross sections of the slope, water table, core recovery and drilling locations.

3.3. Installation of Pillar at Site for deformation data

The pillars were installed in the study area to record the deformation in various season. The co-ordinates of the pillar were taken during the installation and variation of the data in different month were recorded. Total of 16 numbers of pillars were installed in the study area. The recorded deformations were used to back calculate the mobilized parameters. Figure 3.1 shows the location of pillars and the Co-ordinate data was taken with the reference of benchmarks BM1 and BM2 which are fixed points and does not move and any deformation recorded is relative to these fixed benchmarks.T39, T40, T41 represents the transmission line tower location.

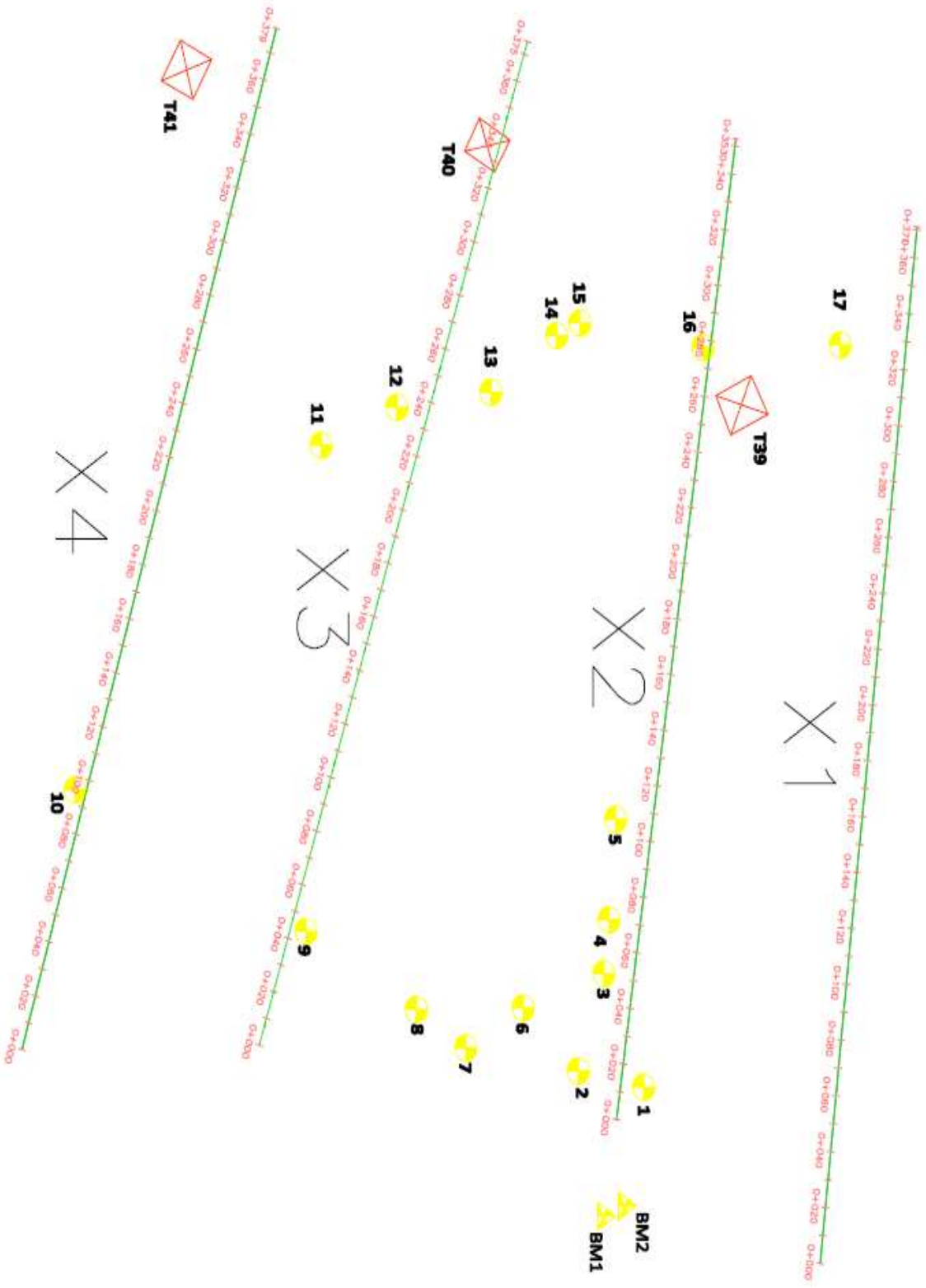

Figure 3. 1: Location of instrumented Pillars (Source: NEA Engineering Co. Ltd.)

Figure 3. 2: Pillar number 10 installed at the study area

3.4. Survey Works

The survey work reports are collected from NEA engineering company limited. In order to perform back analysis, the cross section of the critical slope is needed. The sketch of cross section were provided by the NEA engineering company limited.

Figure 3. 3: Cross section of the studied slope (Source: NEA Engineering Co. Ltd.)

Figure 3. 4: Recording the data of Pillar number 7 using total station at the study area

Cross section X2 as shown in Figure 3.3 is used for the back analysis using deformation data as this slope represent the more number of pillars i.e. Pillar 1, Pillar 2, Pillar 3, Pillar 4, Pillar 5, Pillar 6 and Pillar 16.

3.5. Borehole Drilling Works

The borehole data was obtained from NEA engineering company limited. Borehole drilling was done in two locations as shown in Figure 1.1 represented by BH1 and BH2. In borehole BH1 bed rock of fine grain, slightly weathered, schist with quartz veins are encountered. Some fractures are parallel to drilling axis are present. The rock is foliated and the fracture in the foliation plane consists of undulation. In borehole BH2 pebble-boulder of fine grained slightly weathered schist and coarse grain quartz veins are encountered. No bed rock is encountered up to the depth of 33m during core drilling

works. The cross section of the slope is modelled using the borehole drilling data available. The ground water table is encountered at the depth of 25m at borehole BH2.

3.6. Estimating the Material Properties

As we have the borehole data and deformation data recorded for various seasons, the shear strength parameters are estimated using the FEM software using the Mohr-Coulomb Criteria whose principal have been discussed in Chapter 2.5.

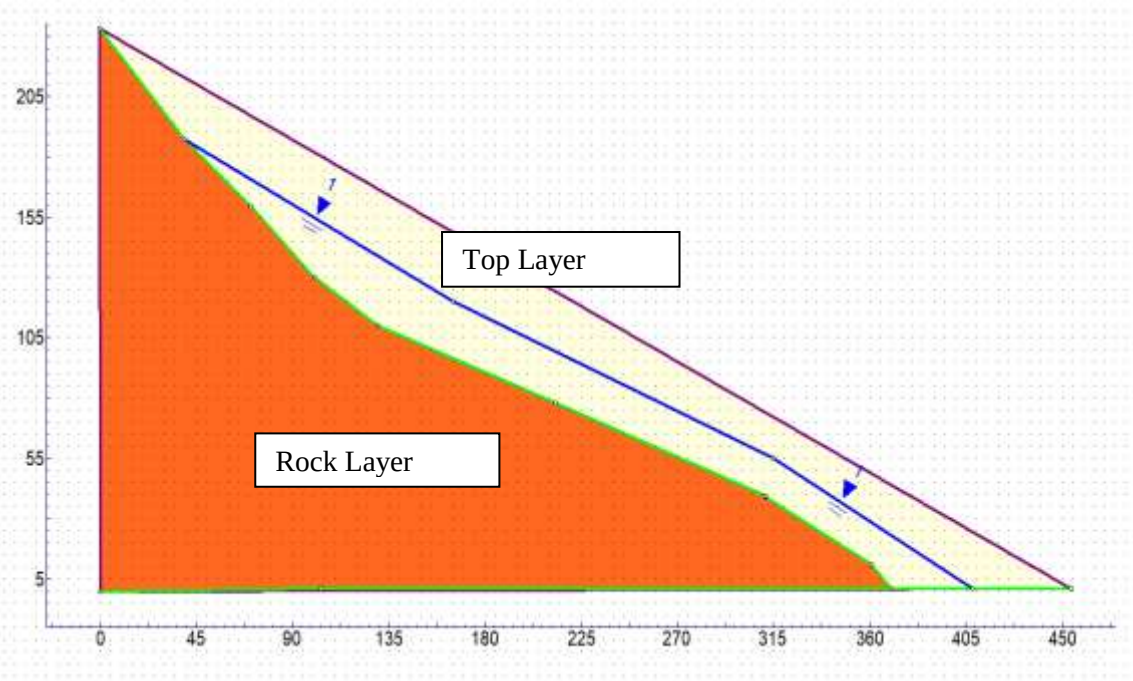

Figure 3. 5: Plot of Cross section with different material boundary and GWT

3.7. Tools used for Modelling

Two tools are used here for the back analysis of the slope. FEM software is used to back calculate the strength parameters using the deformation data obtained from the field using FEM. This obtained parameters are again used for the probabilistic analysis to calculate the Factor of Safety using the software using LEM.

3.7.1. FEM Software

As we have the borehole data and deformation data recorded for various seasons, the shear strength parameters are estimated using the FEM software using FEM. This 2-D software comes up with an easy way to use CAD (Computer Aided Design) based on graphical interface with a wide range of modeling and data interpretation options that

enable users to perform required analysis more thoroughly and more quickly. The cross section obtained from survey is modelled with different boundary for each material and imported in to the software.

3.7.1.1 Steps Requirements for solution of the problem in FEM software

1) Model Geometry
2) External Boundary
3) Material Boundary
4) Piezometric Lines
5) Defining Material Properties
6) Assigning Material Properties
7) Mesh Setup
8) Boundary Conditions
9) Computing the Analysis
10) Interpretation

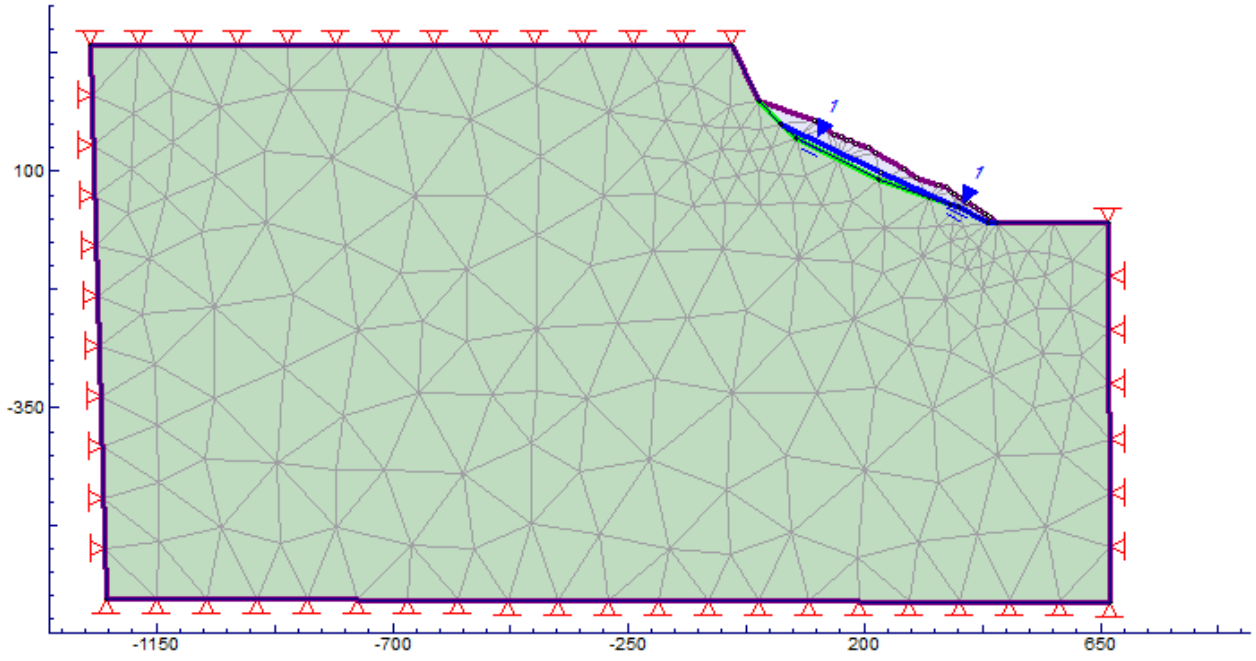

Figure 3. 6: Mesh Set up and restrain in X and Y directions in Model

3.7.2. LEM Software

Slope/ W analysis in LEM software is used to analyze the slope taking the data output received from FEM method.

SLOPE/W uses the limit equilibrium approach to assess the stability of a defined geometry. The limit equilibrium method divides a potential sliding mass, defined by a trial slip surface, into vertical slices. An iterative solution is used to determine the factor by which the shear strength of all slices must be reduced such that the sliding mass is just at the point of static equilibrium (before failure occurs).

This reduction factor is referred to as the factor of safety. Equilibrium can be assessed with respect to moment or force equilibrium. Thus, SLOPE/W computes two factors of safety; one with respect to overall moment equilibrium and one with respect to horizontal force equilibrium. Another iterative solution determines the interslice force factor (lambda; the ratio of the interslice shear and interslice normal forces) generating the same factor of safety for both moment and force equilibrium. (SLOPE/W tutorial).

3.7.2.1 Step requirements for problem solving in LEM software

1) Region
2) Define Material
3) Assign Material
4) Define Analysis
5) Piezometric Surface
6) Slip Surface
7) Running Analysis
8) Results

3.8 Selection of Parameters and Assumptions

The following consideration are made during the selection of parameters and model preparation:

1) It is assumed that the measured deformation in the instrumented pillars to the depth of about 1.5 ft. represent the deformation pattern of the slope. The top layer is overburden material containing granular material, so it is assumed that the whole overburden material represent similar deformation pattern.
2) The deformation in the rock layer is not considered. The roadway area is also considered stiff during preparation of Model.
3) Mohr-Coulomb Model is selected for the granular top layer material. Any model

considered for second layer is not significant for this study as deformation is not studied and considered in this portion.

4) The fixation of parameter in FEM using deformation data was done after varying the parameters in the range as shown in Table 3.1. The range of values of c', ϕ' and ϒ were considered as per the material property considering the borehole log data. The value considered for trial are denoted below:

   Table 3.1: Data range considered for parameter fixation.

Layer	Range of ϒ(kN/M^3)	Range of c'(kPa)	Range of ϕ'(degree)
Top Layer	14-24	0-10	20-35
Rock Layer	20-30	60-100	20-35

5) The vertical displacement in the pillars were taken for the study. The consideration of vertical displacement also includes the displacement in X direction indirectly as displacement in Y direction is seen after the pillar has displaced in X direction. The displacement in X and Y direction can be considered for further study and further research.
6) The recommendation and design for the mitigation measures have the vast scope and could not be incorporated in details as we are only analyzing the performance of the proposed protection system.

3.8. Use of Back Analyzed In-situ parameters

After the development of all the parameters required for numerical modelling through the method developed above, the value of back calculated parameters are used to analyze the stability and mitigation modelling.

Solution to the Slope Stability Problems

After the development of all the parameters required for numerical modelling through the method developed above.

4. Field Measurement

The concrete pillars are installed in the different location in the study area as shown in Figure 4.1. The deformation in the various months are measured by using total station surveying equipment. The measured deformation are compared with the data of the first pillar installed month. The co-ordinates of the installed pillars are recorded after installation with respect to the fixed position benchmark BM2 and BM1. The Co-ordinates of the installed pillars in the month of Falgun is tabulated below in Table 4.1.

Figure 4.1: Location of Installed Pillars in the study area (Source: Google Earth)

Borehole drilling was carried out in the BH1 and BH2 location and the geological log of the bore hole was prepared in the site and is represented in ANNEX section. This borehole log is used to prepare a geological model for the required analysis.

4.1 Field Measurement data during Installation of Pillars

As shown in Figure 4.1, sixteen pillars were installed in the study area and the co-ordinates of the pillars were recorded starting from BM1 and BM2 which are fixed points near the abutment of the Singati Bridge.

Table 4.1. Field measurement data of Falgun month.

S.N.	X	Y	Z	Remarks
1	500000	5000000	500	BM2
2	499957.847	5000008.214	509.804	Pillar
3	499917.418	4999991.381	539.814	Pillar
4	499952.004	4999980.509	516.697	Pillar
5	499862.484	4999996.329	578.388	Pillar
6	499917.413	4999991.363	539.782	Pillar
7	499929.594	4999957.190	532.511	Pillar
8	499902.381	4999865.290	527.876	Pillar
9	499930.078	4999911.986	525.389	Pillar
10	499943.849	4999932.961	520.707	Pillar
11	499851.965	4999767.543	568.547	Pillar
12	499710.512	4999943.561	650.972	Pillar
13	499690.363	4999971.344	655.448	Pillar
14	499693.722	5000091.366	669.69	Pillar
15	499624.785	4999932.436	690.128	Pillar
16	499612.962	4999938.748	693.377	Pillar

4.2 Field Measurement Data during Chaitra Month

Second measurement of pillar data was taken on Chaitra 29th. Survey was carried out starting from the fixed bench marks points and co-ordinates were recorded. Field measurement showed some deformation in all three directions with respect to Falgun Data.

Table 4.2. Field measurement data of Chaitra month.

Pillar No.	X	Y	Z	Remarks
Pillar 1	499957.847	5000008.214	509.77	
Pillar 2	499952.004	4999980.509	516.648	
Pillar 3	499943.849	4999932.961	520.707	
Pillar 4	499930.078	4999911.986	525.382	
Pillar 5	499902.381	4999865.29	527.872	
Pillar 6	499929.594	4999957.19	532.51	
Pillar 7	499917.413	4999991.363	539.789	
Pillar 8	499898.209	4999993.581	552.556	
Pillar 9	499862.484	4999996.329	578.366	
Pillar 10	499729.346	4999871.736	641.323	
Pillar 11	499715.842	4999903.777	643.612	
Pillar 12	499690.363	4999971.344	655.442	
Pillar 13	499685.874	4999981.203	657.253	

4.6 Field Measurement Data during Shrawan Month

Second measurement of pillar data was taken on Shrawan 30th. Survey was carried out starting from the fixed bench marks points and co-ordinates were recorded. Field measurement showed some significant deformation in all three directions with respect to Falgun Data.

Pillar No.	X	Y	Z	Remarks
Pillar 1	499957.9251	5000008.423	509.7072	
Pillar 2	499951.7028	4999980.544	516.6463	
Pillar 3	499943.6936	4999933.285	520.702	
Pillar 4	499929.7746	4999912.436	525.3682	
Pillar 5	499901.6438	4999866.061	527.8583	
Pillar 6	499929.4544	4999957.619	532.5096	
Pillar 7	499917.6673	4999991.985	539.7081	
Pillar 8	499898.3354	4999994.207	552.5503	
Pillar 9	499862.404	4999996.228	578.368	
Pillar 10	499729.406	4999871.706	641.274	
Pillar 11	499715.852	4999903.707	643.54	
Pillar 12	499690.3751	4999971.241	655.408	
Pillar 13	499685.864	4999981.253	657.201	

Table 4.3. Field measurement data of Shrawan month

4.3 Observed Vertical deformation by plotting Z data in various seasons

The X, Y and Z co-ordinates for the month of Falgun, Chaitra and Shrawan are recorded and the deformation seen in the vertical direction in various months with relative to Falgun are calculated and presented in the next sections. The deformation in the Y direction i.e. in the vertical direction which can be seen by plotting the Z co-ordinates measured during various months are presented in the below figures for each Pillar data.

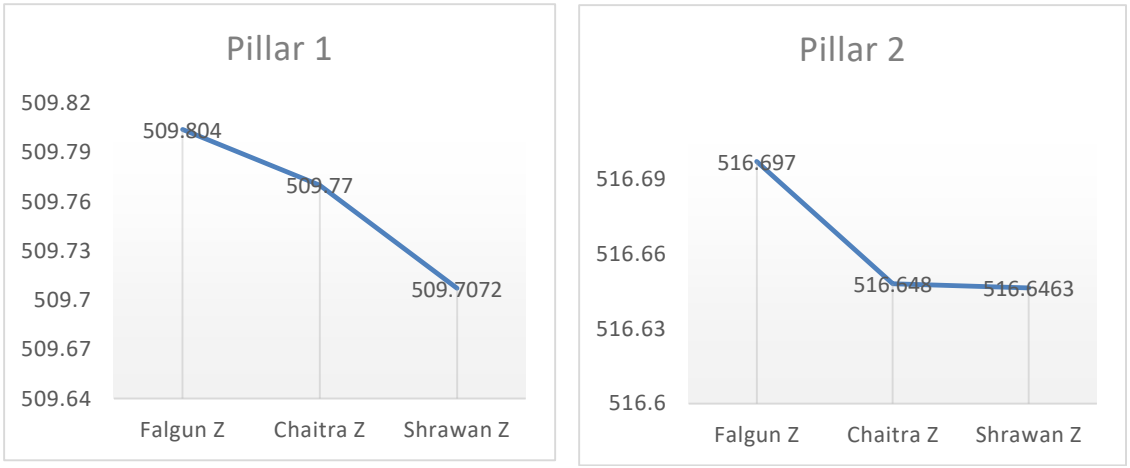

Figure 4.2: Plot of Z value in Pillar 1 and Pillar 2 in various months.

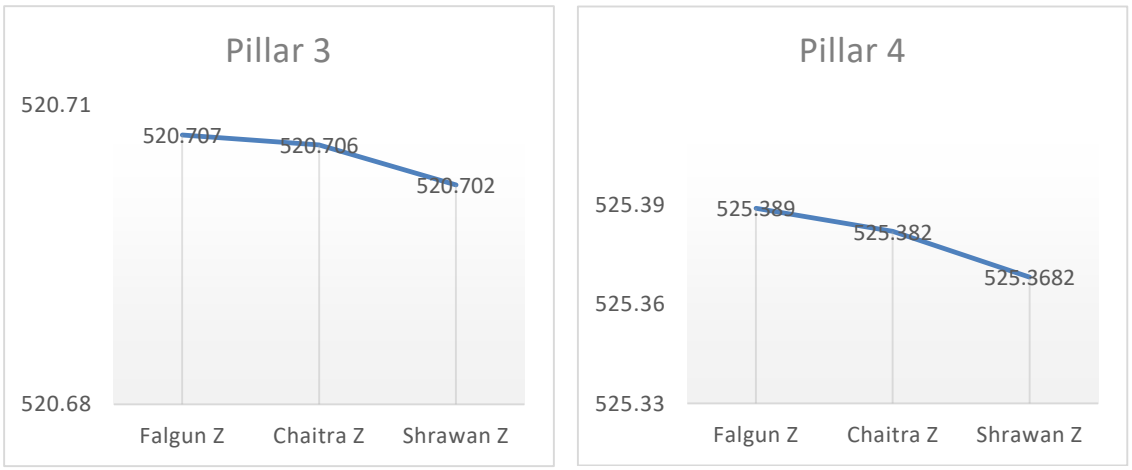

Figure 4.3: Plot of Z value in Pillar 3 and Pillar 4 in various months.

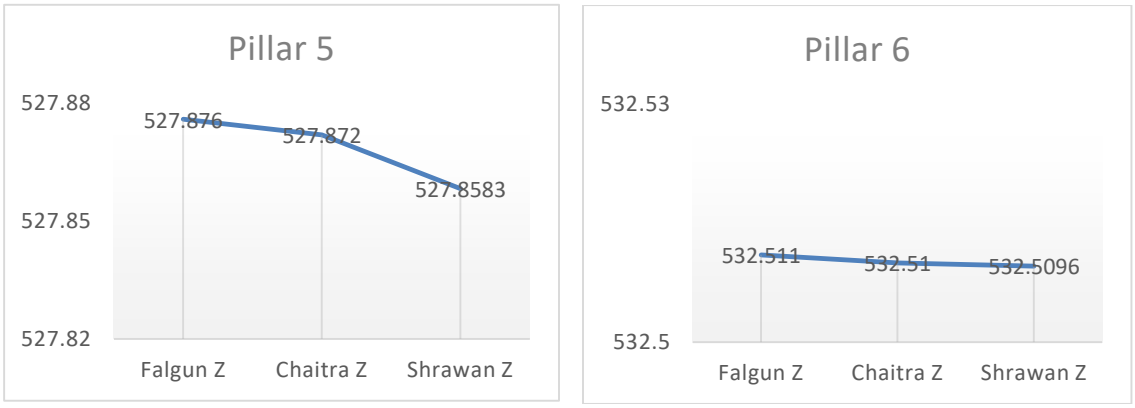

Figure 4.4: Plot of Z value in Pillar 5 and Pillar 6 in various months.

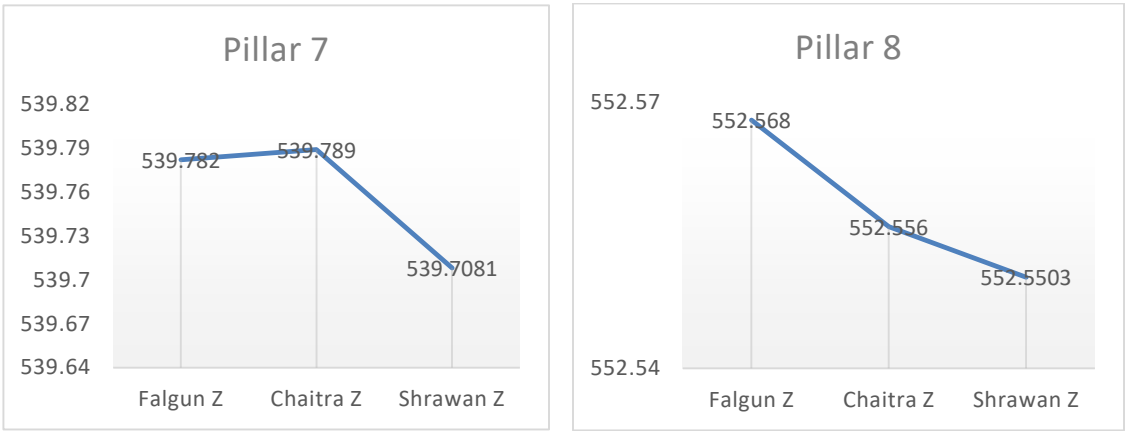

Figure 4.5: Plot of Z value in Pillar 7 and Pillar 8 in various months

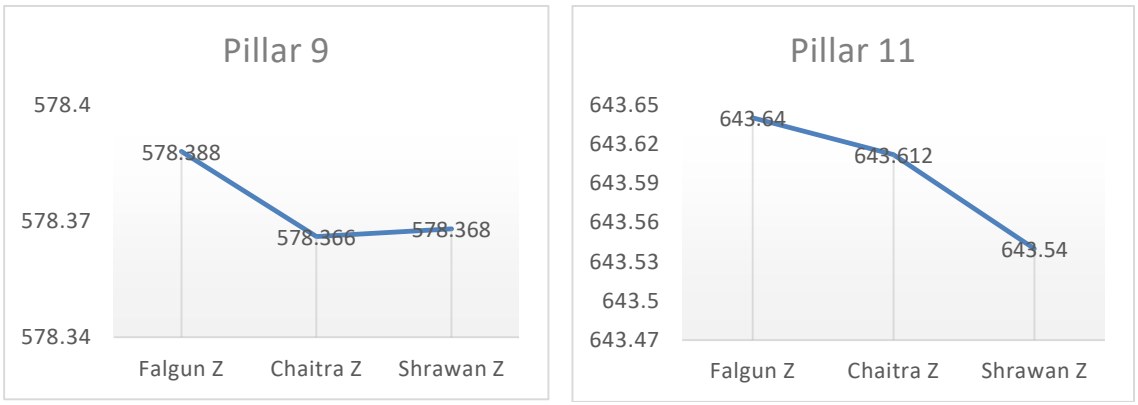

Figure 4.6: Plot of Z value in Pillar 9 and Pillar 11 in various months.

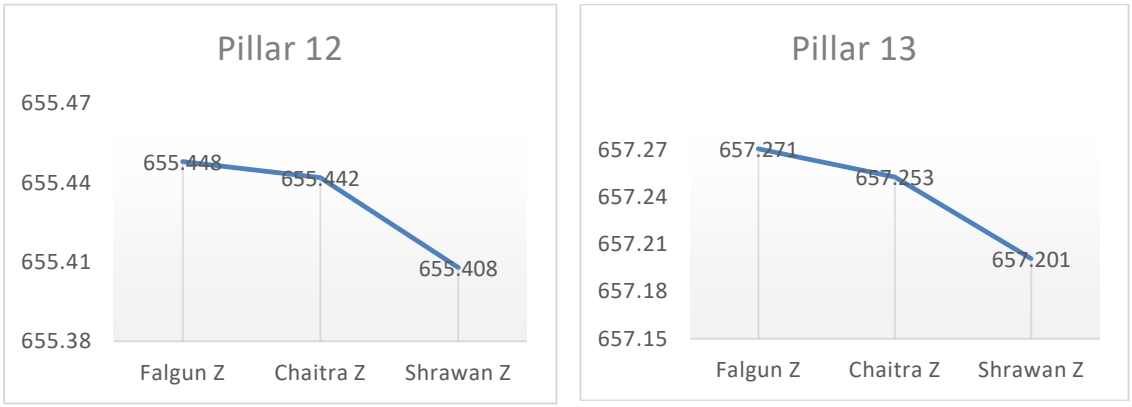

Figure 4.7: Plot of Z value in Pillar 12 and Pillar 13 in various months.

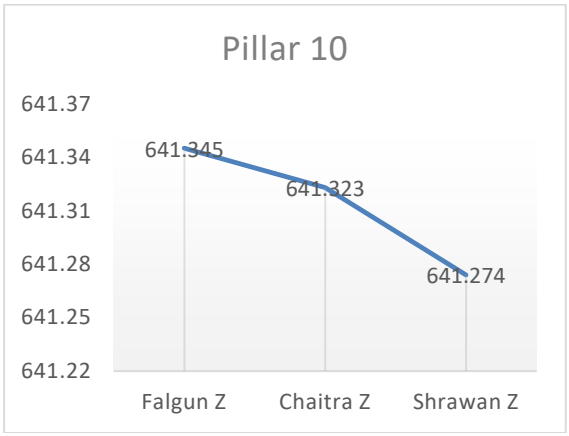

Figure 4.8: Plot of Z value in Pillar 10 in various months.

4.4 Observed Deformation in X direction in study period

The deformation in X direction is calculated with respect to the X co-ordinate data of the Falgun month and the deformation shown below is the deformation in the pillars in the Shrawan month relative to Falgun month data.

Table 4.4. Observed deformation data in X direction in Falgun to Shrawan.

Pillar No.	Falgun X	Shrawan X	Variation Falgun Shrawan	Remarks
Pillar 1	499957.847	499957.9251	-0.0781	
Pillar 2	499952.004	499951.7028	0.3012	
Pillar 3	499943.849	499943.6936	0.1554	
Pillar 4	499930.078	499929.7746	0.3034	
Pillar 5	499902.381	499901.6438	0.7372	
Pillar 6	499929.594	499929.4544	0.1396	
Pillar 7	499917.413	499917.6673	-0.2543	
Pillar 8	499898.209	499898.3354	-0.1264	
Pillar 9	499862.484	499862.404	0.08	
Pillar 10	499729.346	499729.406	-0.06	
Pillar 11	499715.842	499715.852	-0.01	
Pillar 12	499690.363	499690.3751	-0.0121	
Pillar 13	499685.874	499685.864	0.01	

4.5 Observed Deformation in Y direction in study period

The deformation in Y direction is calculated with respect to the Y co-ordinate data of the Falgun month and the deformation shown below is the deformation in the pillars in Y direction in the Shrawan month with respect to Falgun month data.

Table 4.5. Observed deformation data in Y direction in Falgun to Shrawan

Pillar No.	Falgun Y	Shrawan Y	Variation Falgun Shrawan	Remarks
Pillar 1	5000008.214	5000008.423	-0.209	
Pillar 2	4999980.509	4999980.544	-0.035	
Pillar 3	4999932.961	4999933.285	-0.324	
Pillar 4	4999911.986	4999912.436	-0.450	
Pillar 5	4999865.29	4999866.061	-0.771	
Pillar 6	4999957.19	4999957.619	-0.429	
Pillar 7	4999991.363	4999991.985	-0.622	
Pillar 8	4999993.581	4999994.207	-0.626	
Pillar 9	4999996.329	4999996.228	0.101	
Pillar 10	4999871.736	4999871.706	0.030	
Pillar 11	4999903.777	4999903.707	0.070	
Pillar 12	4999971.344	4999971.241	0.103	
Pillar 13	4999981.203	4999981.253	-0.050	

4.7 Variation of X in Chaitra to Shrawan Month

The deformation in X direction is calculated with respect to the X co-ordinate data of the Chaitra month and the deformation shown below is the deformation in the pillars in the Shrawan month relative to Chaitra month data.

Table 4.6. Observed deformation data in X direction in Chaitra to Shrawan.

Pillar No.	Chaitra X	Shrawan X	Variation Chaitra Shrawan
Pillar 1	499957.847	499957.9251	-0.0781
Pillar 2	499952.004	499951.7028	0.3012
Pillar 3	499943.849	499943.6936	0.1554
Pillar 4	499930.078	499929.7746	0.3034
Pillar 5	499902.381	499901.6438	0.7372
Pillar 6	499929.594	499929.4544	0.1396
Pillar 7	499917.413	499917.6673	-0.2543
Pillar 8	499898.209	499898.3354	-0.1264
Pillar 9	499862.484	499862.404	0.08
Pillar 10	499729.346	499729.406	-0.06
Pillar 11	499715.842	499715.852	-0.01
Pillar 12	499690.363	499690.3751	-0.0121
Pillar 13	499685.874	499685.864	0.01

4.8 Variation of Y in Chaitra to Shrawan Month

The deformation in Y direction is calculated with respect to the Y co-ordinate data of the Chaitra month and the deformation shown below is the deformation in the pillars in Y direction in the Shrawan month with respect to Chaitra month data.

Table 4.7. Observed deformation data in Y direction in Chaitra to Shrawan

Pillar No.	Chaitra Y	Shrawan Y	Variation Chaitra Shrawan
Pillar 1	5000008.214	5000008.423	-0.209
Pillar 2	4999980.509	4999980.544	-0.035
Pillar 3	4999932.961	4999933.285	-0.324
Pillar 4	4999911.986	4999912.436	-0.450
Pillar 5	4999865.29	4999866.061	-0.771
Pillar 6	4999957.19	4999957.619	-0.429
Pillar 7	4999991.363	4999991.985	-0.622
Pillar 8	4999993.581	4999994.207	-0.626
Pillar 9	4999996.329	4999996.228	0.101
Pillar 10	4999871.736	4999871.706	0.030
Pillar 11	4999903.777	4999903.707	0.070
Pillar 12	4999971.344	4999971.241	0.103
Pillar 13	4999981.203	4999981.253	-0.050

4.9 Observed deformation in Z direction in dry period

The deformation in Z direction is calculated with respect to the Z co-ordinate data of the Falgun month and the deformation shown below is the deformation in the pillars in Z direction in the Chaitra month with respect to Falgun month data.

Table 4.8. Observed deformation data in Z direction in Falgun to Chaitra

Pillar No.	Falgun Z	Chaitra Z	Variation Falgun Chaitra
Pillar 1	509.804	509.77	0.034
Pillar 2	516.697	516.648	0.049
Pillar 3	520.707	520.706	0.001
Pillar 4	525.389	525.382	0.007
Pillar 5	527.876	527.872	0.004
Pillar 6	532.511	532.51	0.001
Pillar 7	539.782	539.789	-0.007
Pillar 8	552.568	552.556	0.012
Pillar 9	578.388	578.366	0.022
Pillar 10	641.345	641.323	0.022
Pillar 11	643.64	643.612	0.028
Pillar 12	655.448	655.442	0.006
Pillar 13	657.271	657.253	0.018

4.10 Observed deformation in Z direction in wet period

The deformation in Z direction is calculated with respect to the Z co-ordinate data of the Chaitra month and the deformation shown below is the deformation in the pillars in Z direction in the Shrawan month with respect to Chaitra month data.

Table 4.9. Observed deformation data in Z direction in Chaitra to Shrawan

Pillar No.	Chaitra Z	Shrawan Z	Variation Chaitra Shrawan
Pillar 1	509.77	509.7072	0.0628
Pillar 2	516.648	516.6463	0.0017
Pillar 3	520.706	520.702	0.004
Pillar 4	525.382	525.3682	0.0138
Pillar 5	527.872	527.8583	0.0137
Pillar 6	532.51	532.5096	0.0004
Pillar 7	539.789	539.7081	0.0809
Pillar 8	552.556	552.5503	0.0057
Pillar 9	578.366	578.368	-0.002
Pillar 10	641.323	641.274	0.049
Pillar 11	643.612	643.54	0.072
Pillar 12	655.442	655.408	0.034
Pillar 13	657.253	657.201	0.052

4.11 Discussion on the field measurement data

The field measurement data were presented and calculations for the deformation in the dry season and in the wet season were made. Dry season is represented by Falgun-Chaitra period and wet season is represented by Chaitra- Shrawan period in this study period.

The plot of Y co-ordinate data in different months were presented in the chart as shown in Figure 4.2, Figure 4.3, Figure 4.4, Figure 4.5, Figure 4.6, Figure 4.7 and Figure 4.8. Pillar 1, Pillar 3, Pillar 4, Pillar 5, Pillar 8, Pillar 10, Pillar 11, Pillar 12 and Pillar 13 showed the similar vertical deformation pattern for dry as well as wet season. The rate of deformation obtained is less in the dry season and increase in rate of vertical deformation can be seen clearly in the case of wet season.

In case of Pillar 1, the vertical deformation of 34 mm is seen in the dry season period and the vertical deformation of 62.8 mm in the wet season. In case of Pillar 5, the vertical deformation of 4mm is seen in the dry season period and the vertical deformation of 13.7 mm in the wet season. The Figure 4.9 shows the vertical deformation pattern and deformation values in different seasons.

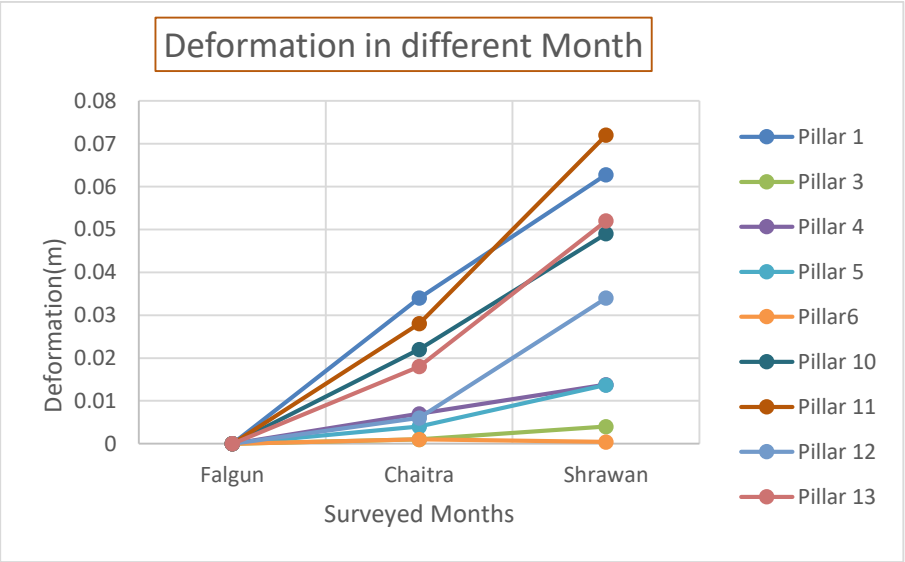

Figure 4.9: Vertical deformation in various seasons.

The vertical deformation in the lower part of slope i.e. in case of Pillar 1, Pillar 2 and Pillar 7 showed higher deformation value, the portion having the Pillar 4 and Pillar 5 showed lesser deformation and again the portion having the Pillar 16 shows the maximum vertical deformation.

5. Numerical Modelling and Results

After completion of the field measurements the numerical modelling for problem solving was carried out. Model was prepared using the cross section data obtained from the survey and the geological log of drill hole in BH1 and BH2 location. The methodology presented in Chapter 3 of this thesis report is followed to carry out numerical modelling and obtain the results.

FEM was carried out to back calculate the strength parameters using the deformation data obtained from the field measurements. Two layer material model is prepared using the field measurement data. Top layer and Rock Layer names were assigned to two different layers. The external boundaries were assigned and the restrains as per the field conditions were applied in the model. Discretization and mesh set up were completed and different assumed values for the material properties were assigned. After the model is completed, it is calculated to obtain the results. The number of trials assigning the different values of c', ϕ', Υ and varying the different depths of water table for obtaining the field recorded deformation in the model were carried out. The major trials and there results are presented in this section.

After back calculating the strength parameters and water table depths, the model is prepared in LEM using these data to calculate the Factor of Safety Values. The different LEM trials are carried out and the results obtained are presented in this section.

The results obtained in this section are discussed in the next Chapter of this thesis report and used for the mitigation of the problems.

The model and results of the trials which are not incorporated in this section are presented in the Annex Section of this thesis report.

5.1 Model in FEM software using borehole log

The model using the cross section from survey and bore hole log data is prepared and various values of c', ϕ' and ϒ are used for the trial to get the deformation pattern obtained in the field. After the deformation pattern is matched for those values of c', ϕ' and ϒ, the water table is varied by increasing the height of peizometric lines to obtain the deformation recorded in the field.

The geological model presented in Figure 5.1 is prepared using FEM model and this model is used as the base model for the number of trails carried out. The restrains as per site condition is provided in the model.

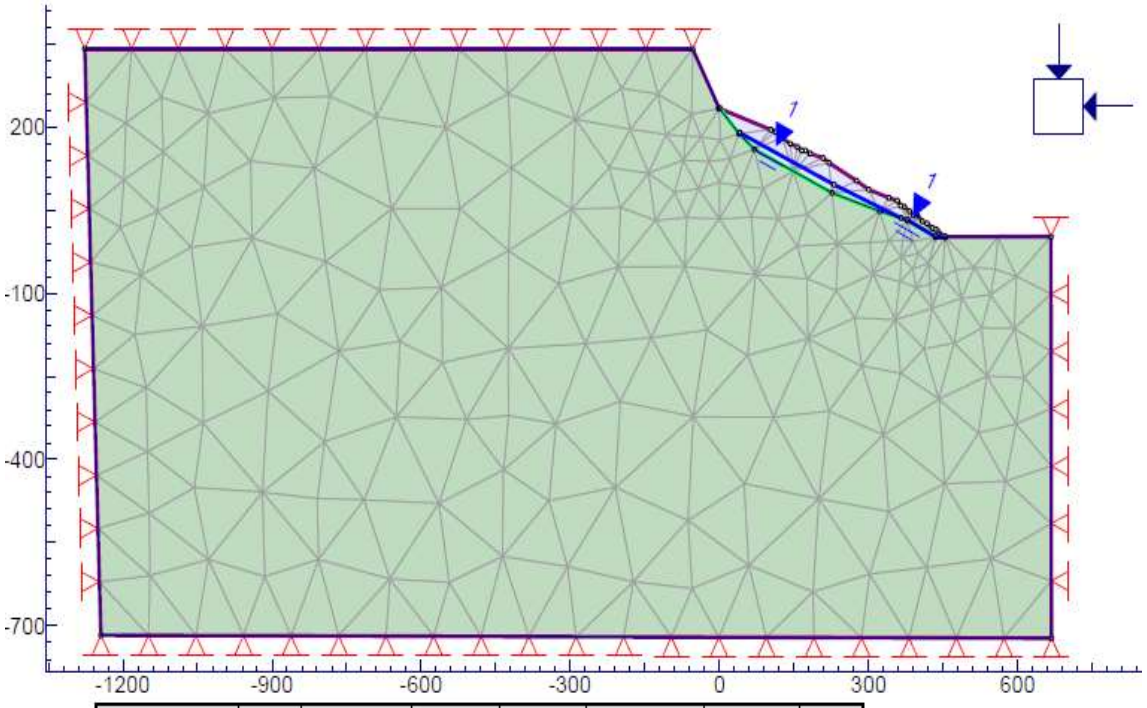

Material Name	Color	Unit Weight (kN/m3)	Failure Criterion	Material Type	Friction Angle (peak) (deg)	Cohesion (peak) (kPa)	Piezo Line
Top Layer		18	Mohr Coulomb	Elastic	28	5	1
Rock Layer		24	Mohr Coulomb	Elastic	30	85	None

Figure 5. 1: Model in FEM for deformation back analysis.

5.2 Vertical Deformation after 1m rise in water table

The model prepared as in Figure 5.1 is used for this trial with some variations. After the values of c', ϕ' and ϒ are finalized as shown in Figure 5.1 which shows the matching deformation pattern as obtained in field, the next trial is started increasing the water table by 1m to match the deformation obtained from the field measurement. The values c' = 5 kPa, ϕ' = 28˚ and ϒ = 18 kN/m^3 is used for the top layer material properties and the values c' = 85 kPa, ϕ' = 30˚ and ϒ = 24 kN/m^3 are used for the rock layer material properties. The model is computed and the result for vertical deformation is checked and presented here in Figure 5.2. The different deformation zones are represented by the contours and values are presented in the left section in meters. The result obtained here is discussed in the next Chapter of this thesis report.

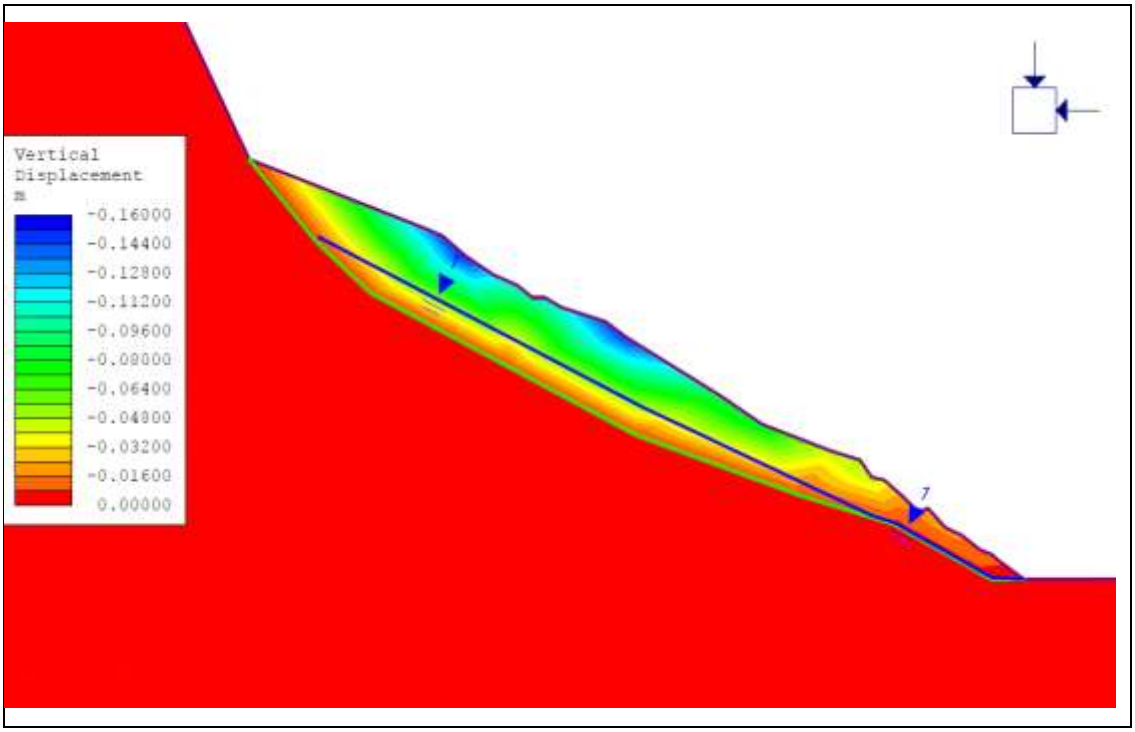

Figure 5. 2: Result for vertical deformation after 1m rise in water table.

5.3 Vertical Deformation after 3m rise in water table

The model prepared as in Figure 5.1 is used for this trial with some variations. After the values of c', ϕ' and ϒ are finalized as shown in Figure 5.1 which shows the matching deformation pattern as obtained in field, the next trial is started increasing the water table by 2m of the original water table to match the deformation obtained from the field measurement. The values c' = 5 kPa, ϕ' = 28˚ and ϒ = 18 kN/m^3 is used for the top layer material properties and the values c' = 85 kPa, ϕ' = 30˚ and ϒ = 24 kN/m^3 are used for the rock layer material properties. The model is computed and the result for vertical deformation is checked and presented here in Figure 5.3. The different deformation zones are represented by the contours and values are presented in the left section in meters. The result obtained here is discussed in the next Chapter of this thesis report.

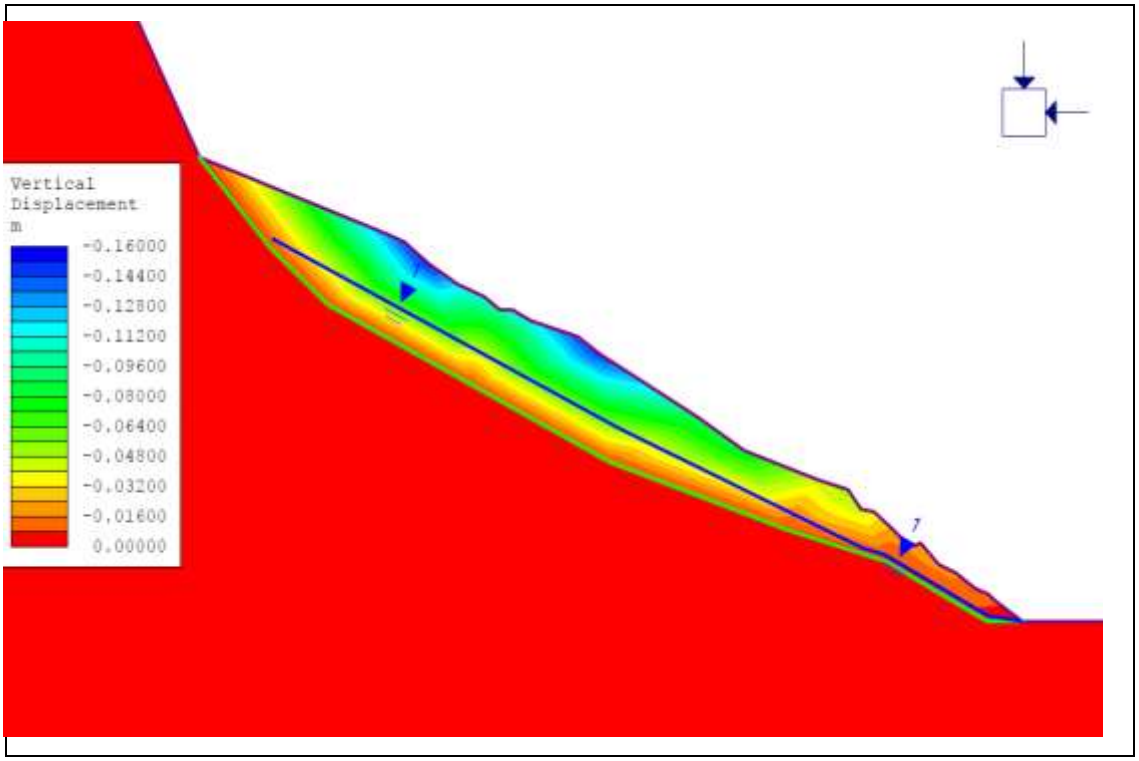

Figure 5. 3: Result for vertical deformation after 3m rise in water table.

5.4 Vertical Deformation after 4m rise in water table

The model prepared as in Figure 5.1 is used for this trial with some variations. After the values of c', ϕ' and ϒ are finalized as shown in Figure 5.1 which shows the matching deformation pattern as obtained in field, the next trial is started increasing the water table by 4m of the original water table to match the deformation obtained from the field measurement. The values c' = 5 kPa, ϕ' = 28˚ and ϒ = 18 kN/m^3 is used for the top layer material properties and the values c' = 85 kPa, ϕ' = 30˚ and ϒ = 24 kN/m^3 are used for the rock layer material properties. The model is computed and the result for vertical deformation is checked and presented here in Figure 5.4. The different deformation zones are represented by the contours and values are presented in the left section in meters. The result obtained here is discussed in the next Chapter of this thesis report.

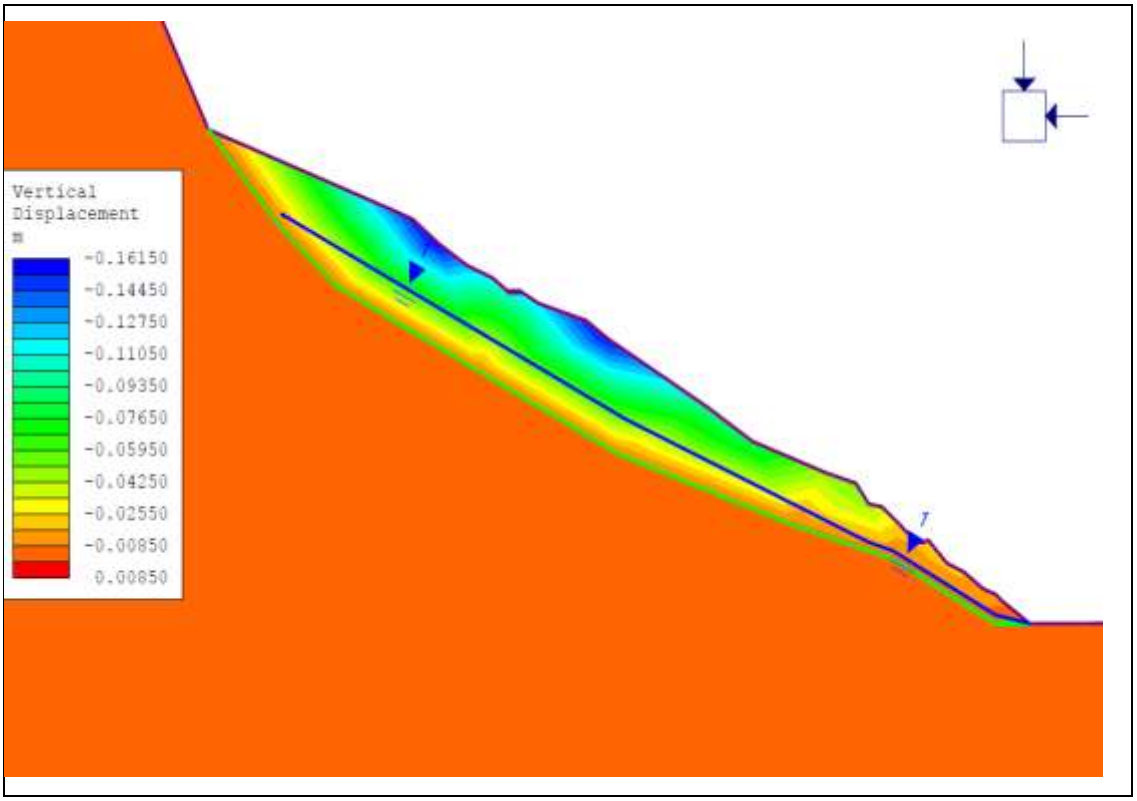

Figure 5. 4: Result for vertical deformation after 4m rise in water table.

5.5 Vertical Deformation after 5m rise in water table

The model prepared as in Figure 5.1 is used for this trial with some variations. After the values of c', ϕ' and ϒ are finalized as shown in Figure 5.1 which shows the matching deformation pattern as obtained in field, the next trial is started increasing the water table by 5m of the original water table to match the deformation obtained from the field measurement. The values c' = 5 kPa, ϕ' = 28˚ and ϒ = 18 kN/m^3 is used for the top layer material properties and the values c' = 85 kPa , ϕ' = 30˚ and ϒ = 24 kN/m^3 are used for the rock layer material properties. The model is computed and the result for vertical deformation is checked and presented here in Figure 5.5. The different deformation zones are represented by the contours and values are presented in the left section in meters. The result obtained here is discussed in the next Chapter of this thesis report.

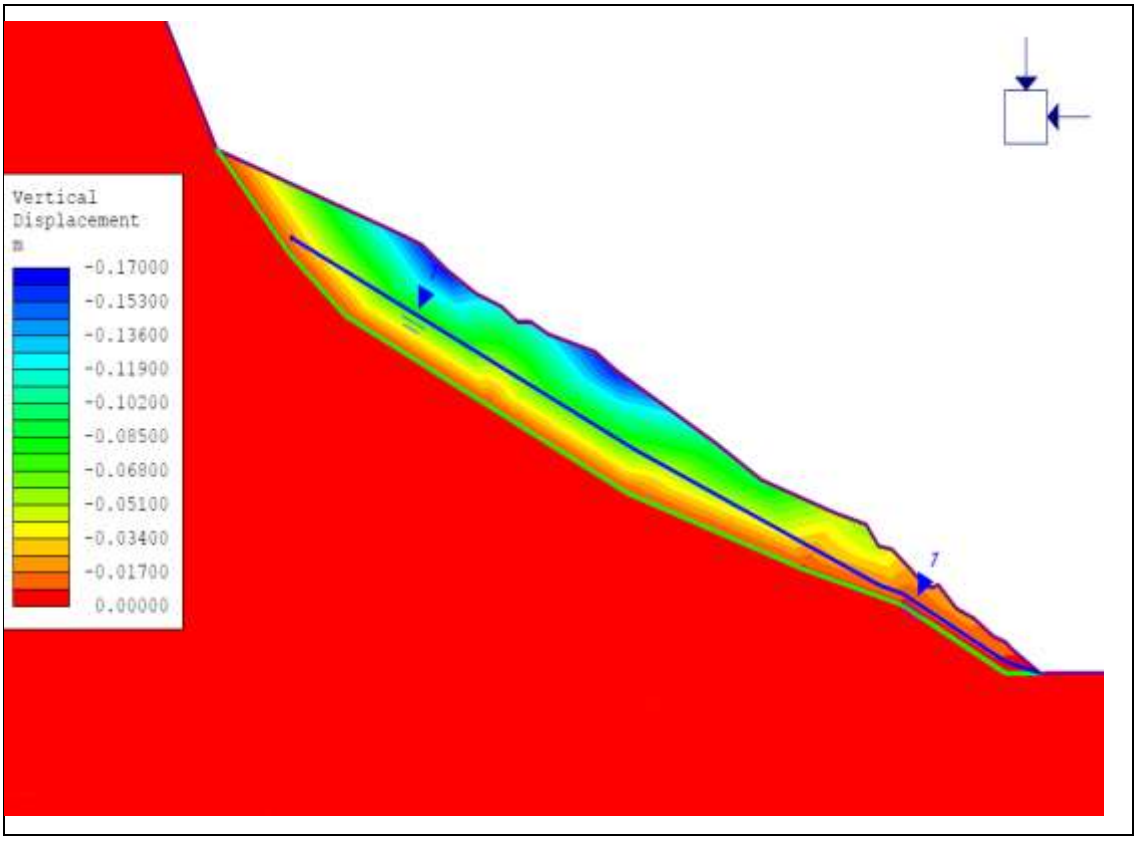

Figure 5. 5: Result for vertical deformation after 5m rise in water table.

5.6 Vertical Deformation after 6m rise in water table

The model prepared as in Figure 5.1 is used for this trial with some variations. After the values of c', ϕ' and ϒ are finalized as shown in Figure 5.1 which shows the matching deformation pattern as obtained in field, the next trial is started increasing the water table by 6m of the original water table to match the deformation obtained from the field measurement. The values c' = 5 kPa, ϕ' = 28˚ and ϒ = 18 kN/m^3 is used for the top layer material properties and the values c' = 85 kPa, ϕ' = 30˚ and ϒ = 24 kN/m^3 are used for the rock layer material properties. The model is computed and the result for vertical deformation is checked and presented here in Figure 5.6. The different deformation zones are represented by the contours and values are presented in the left section in meters. The result obtained here is discussed in the next Chapter of this thesis report.

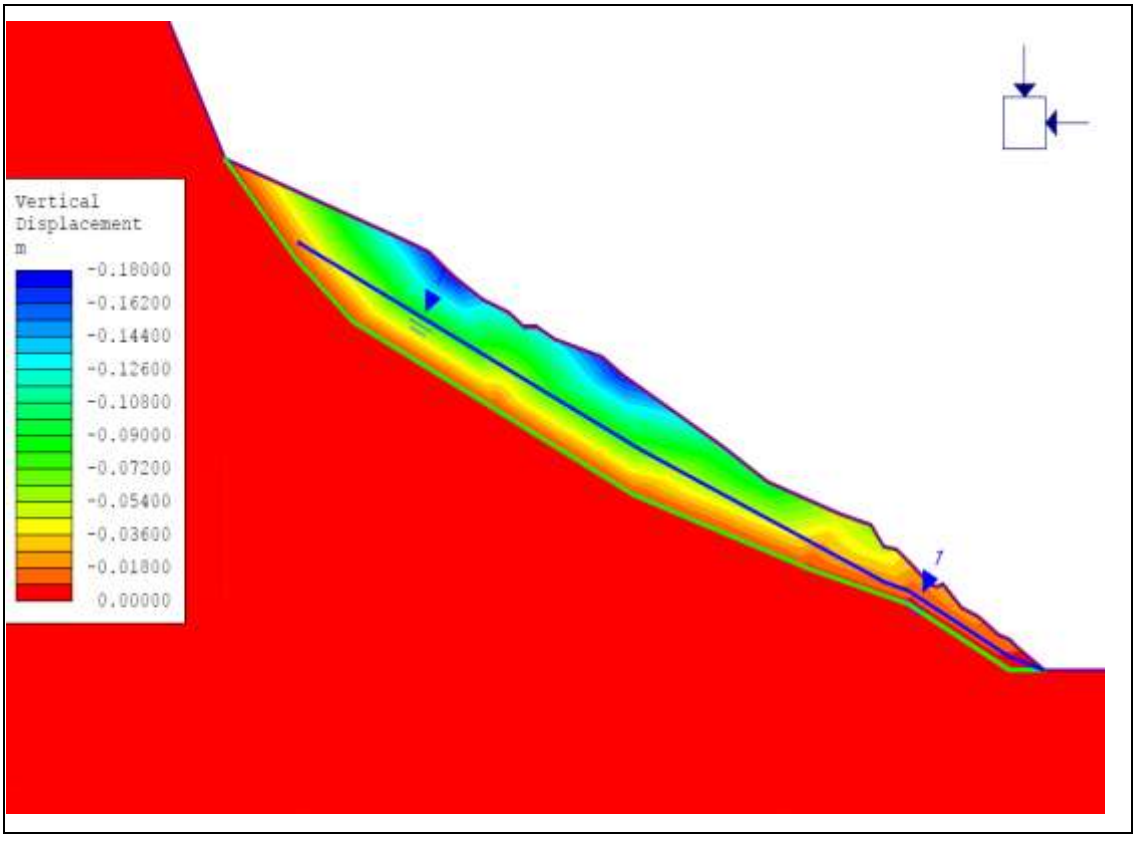

Figure 5. 6: Result for vertical deformation after 6m rise in water table.

5.7 Vertical Deformation after 7m rise in water table

The model prepared as in Figure 5.1 is used for this trial with some variations. After the values of c', ϕ' and ϒ are finalized as shown in Figure 5.1 which shows the matching deformation pattern as obtained in field, the next trial is started increasing the water table by 7m of the original water table to match the deformation obtained from the field measurement. The values c' = 5 kPa, ϕ' = 28˚ and ϒ = 18 kN/m^3 is used for the top layer material properties and the values c' = 85 kPa, ϕ' = 30˚ and ϒ = 24 kN/m^3 are used for the rock layer material properties. The model is computed and the result for vertical deformation is checked and presented here in Figure 5.7. The different deformation zones are represented by the contours and values are presented in the left section in meters. The result obtained here is discussed in the next Chapter of this thesis report.

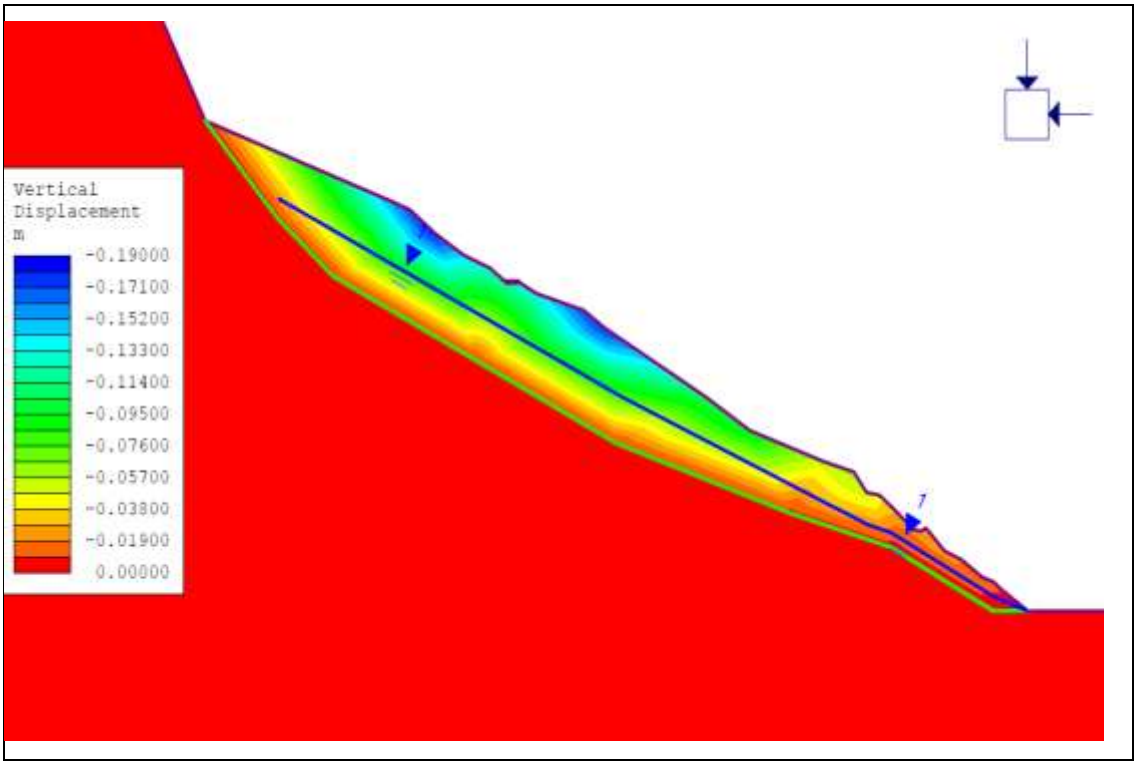

Figure 5. 7: Result for vertical deformation after 7m rise in water table.

5.8 Vertical Deformation after 8m rise in water table

The model prepared as in Figure 5.1 is used for this trial with some variations. After the values of c', ϕ' and ϒ are finalized as shown in Figure 5.1 which shows the matching deformation pattern as obtained in field, the next trial is started increasing the water table by 8m of the original water table to match the deformation obtained from the field measurement. The values c' = 5 kPa, ϕ' = 28˚ and ϒ = 18 kN/m^3 is used for the top layer material properties and the values c' = 85 kPa, ϕ' = 30˚ and ϒ = 24 kN/m^3 are used for the rock layer material properties. The model is computed and the result for vertical deformation is checked and presented here in Figure 5.8. The different deformation zones are represented by the contours and values are presented in the left section in meters. The result obtained here is discussed in the next Chapter of this thesis report.

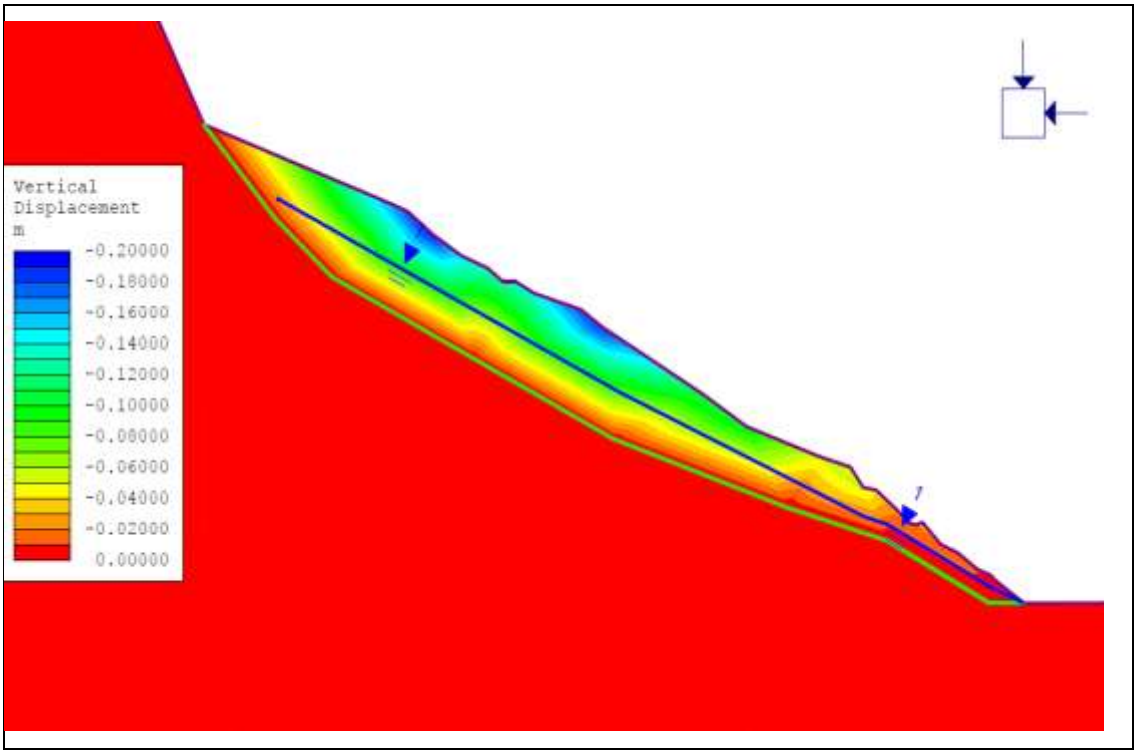

Figure 5. 8: Result for vertical deformation after 8m rise in water table.

5.9 Horizontal deformation after 8m rise in water table

The horizontal deformation computed for the trial after increasing the water table by 8m of the original water table surface is presented in the Figure 5.9.

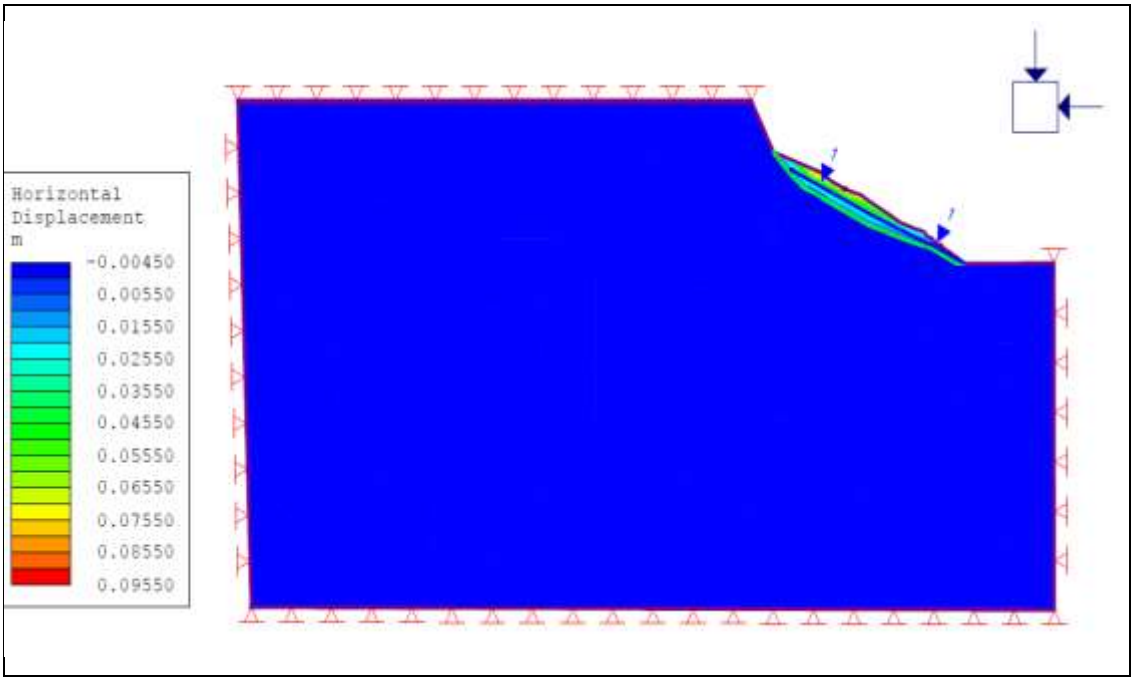

Figure 5. 9: Result for horizontal deformation after 8m rise in water table.

5.10 Total deformation after 8m rise in water table

The total displacement computed for the trial after increasing the water table by 8m of the original water table surface is presented in the Figure 5.10.

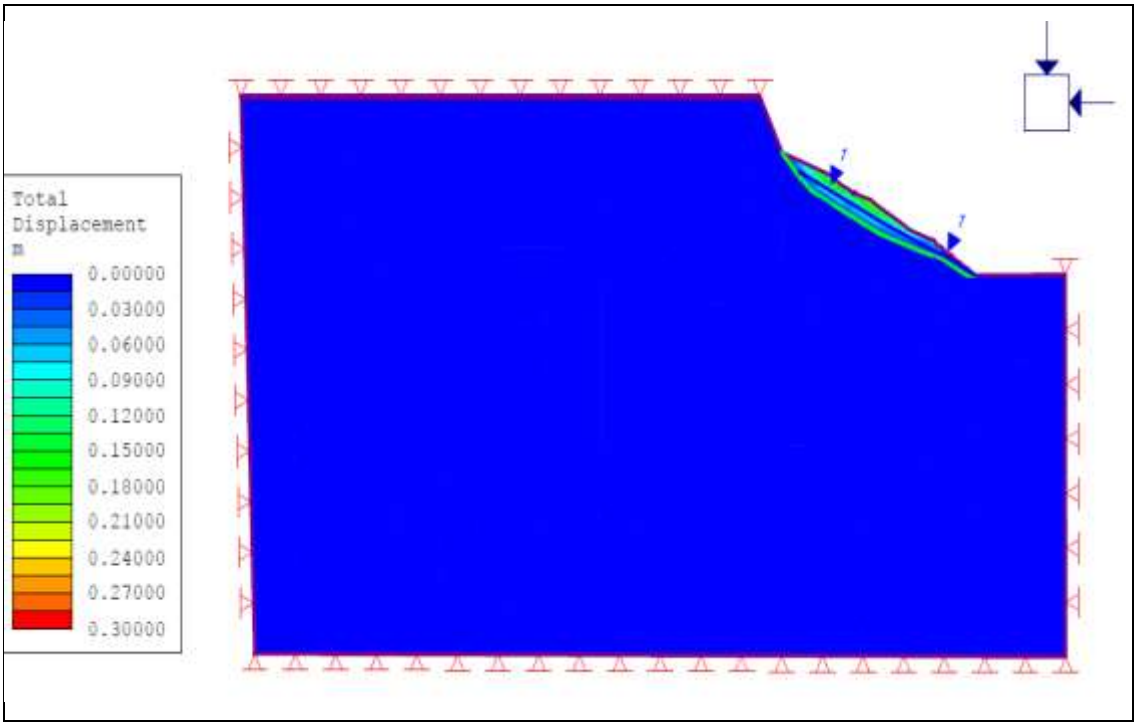

Figure 5. 10: Result for total deformation after 8m rise in water table.

5.11 Vertical Deformation after 9m rise in water table

The model prepared as in Figure 5.1 is used for this trial with some variations. After the values of c', ϕ' and ϒ are finalized as shown in Figure 5.1 which shows the matching deformation pattern as obtained in field, the next trial is started increasing the water table by 9m of the original water table to match the deformation obtained from the field measurement. The values c' = 5 kPa, ϕ' = 28˚ and ϒ = 18 kN/m^3 is used for the top layer material properties and the values c' = 85 kPa, ϕ' = 30˚ and ϒ = 24 kN/m^3 are used for the rock layer material properties. The model is computed and the result for vertical deformation is checked and presented here in Figure 5.9. The different deformation zones are represented by the contours and values are presented in the left section in meters. The result obtained here is discussed in the next Chapter of this thesis report.

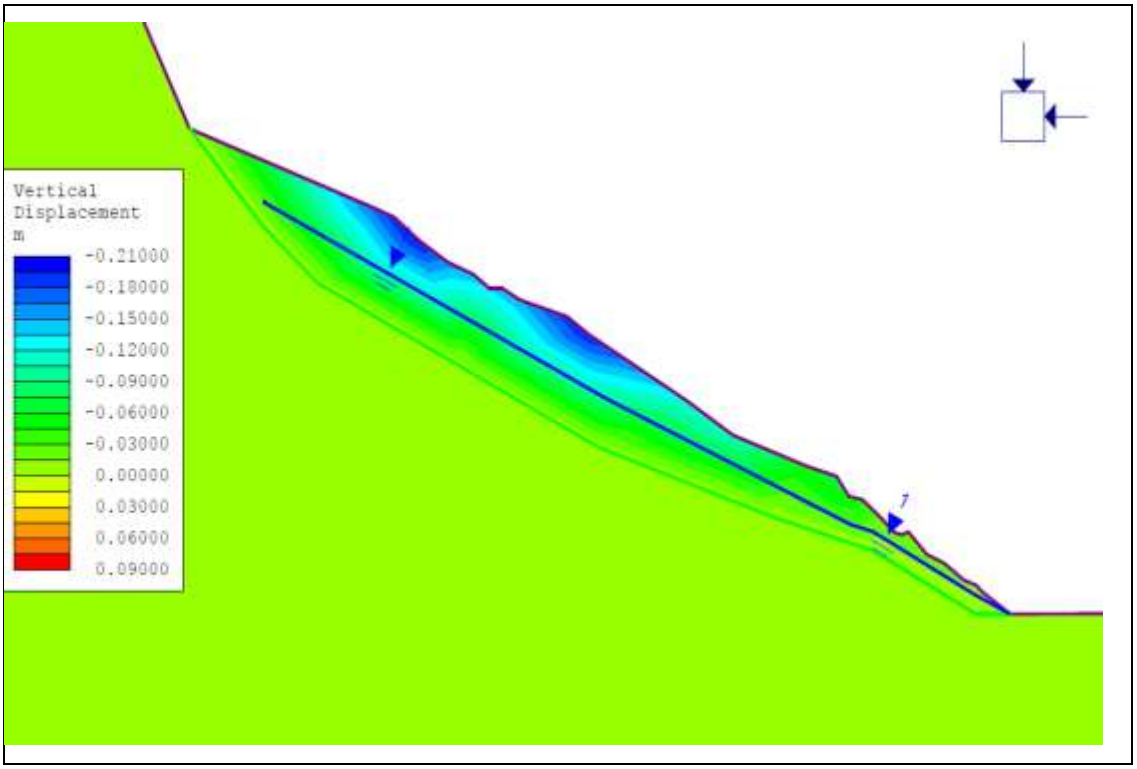

Figure 5. 11: Result for vertical deformation after 9m rise in water table.

5.12 Vertical Deformation after 10m rise in water table

The geological model prepared as in Figure 5.1 is used for this trial with some variations. After the values of c', ϕ' and ϒ are finalized as shown in Figure 5.1 which shows the matching deformation pattern as obtained in field, the next trial is started increasing the water table by 10m of the original water table to match the deformation obtained from the field measurement. The values c' = 5 kPa, ϕ' = 28˚ and ϒ = 18 kN/m^3 is used for the top layer material properties and the values c' = 85 kPa, ϕ' = 30˚ and ϒ = 24 kN/m^3 are used for the rock layer material properties. The model is computed and the result for vertical deformation is checked and presented here in Figure 5.12. The different deformation zones are represented by the contours and values are presented in the left section in meters. The result obtained here is discussed in the next Chapter of this thesis report.

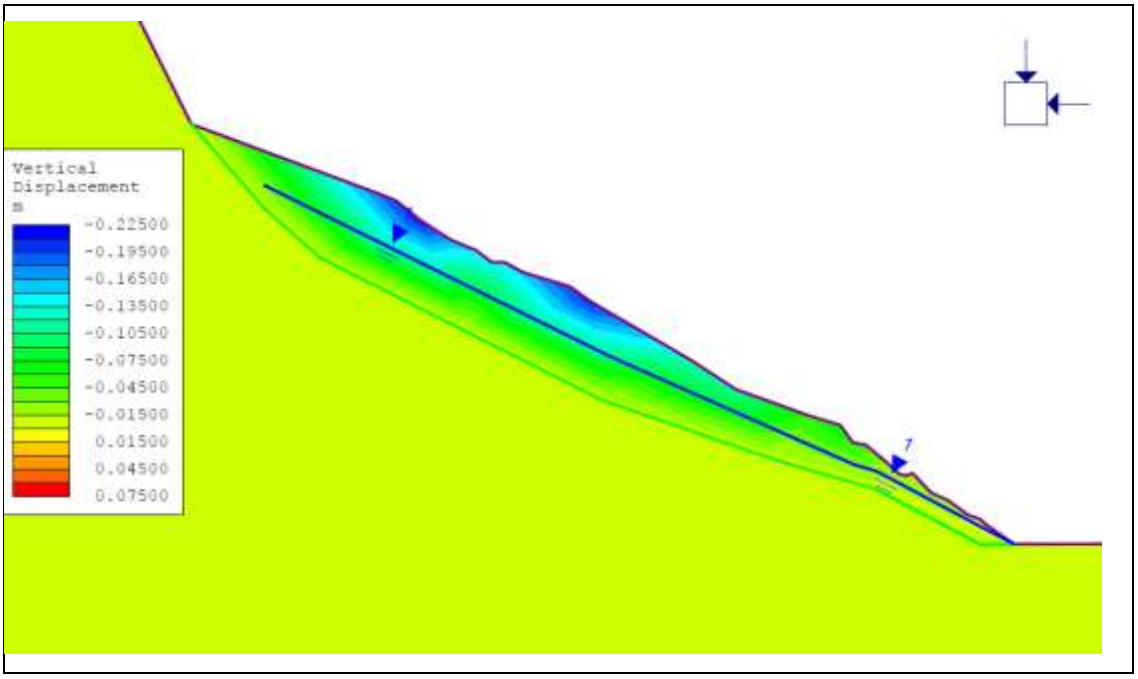

Figure 5. 12: Result for vertical deformation after 10m rise in water table.

5.13 Model in LEM for FOS determination

The back calculated model parameters with the recorded deformation by using FEM is again modelled in LEM to calculate the Factor of Safety of the modelled slope. The calculated value is discussed and further trials and analysis are carried out to give the mitigation of the slope stability problems. The mitigation models are prepared in LEM and suggested for the implementation.

Figure 5.13 shows the geological model prepared in LEM and the data shown in the figure are taken from the back analysis by FEM.

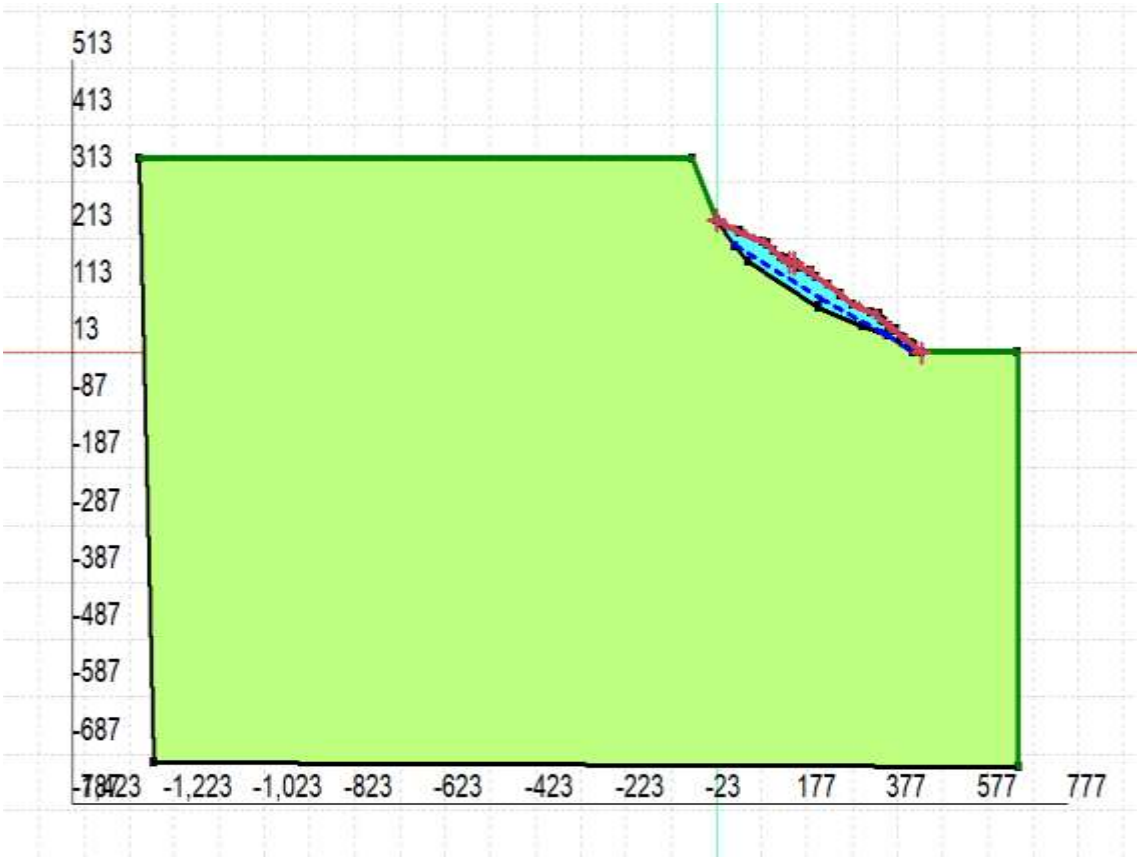

Figure 5. 13: Model in LEM.

5.14 FOS at 8m rise in water table

The back calculated model parameters with the recorded deformation by using FEM is again modelled in LEM as shown in Figure 5.14. The back calculated strength parameters values c' = 5 kPa, ϕ' = 28˚ and ϒ = 18 kN/m^3 is used for the top layer material properties and the values c' = 85 kPa, ϕ' = 30˚ and ϒ = 24 kN/m^3 are used for the rock layer material properties at the water table rise of 8m from the original ground table are used for slope stability analysis.

The material properties are assigned to each layer, entry and exit method is used to represent failure surface. The water table surface at 8m from the original water table is drawn and the analysis is carried out.

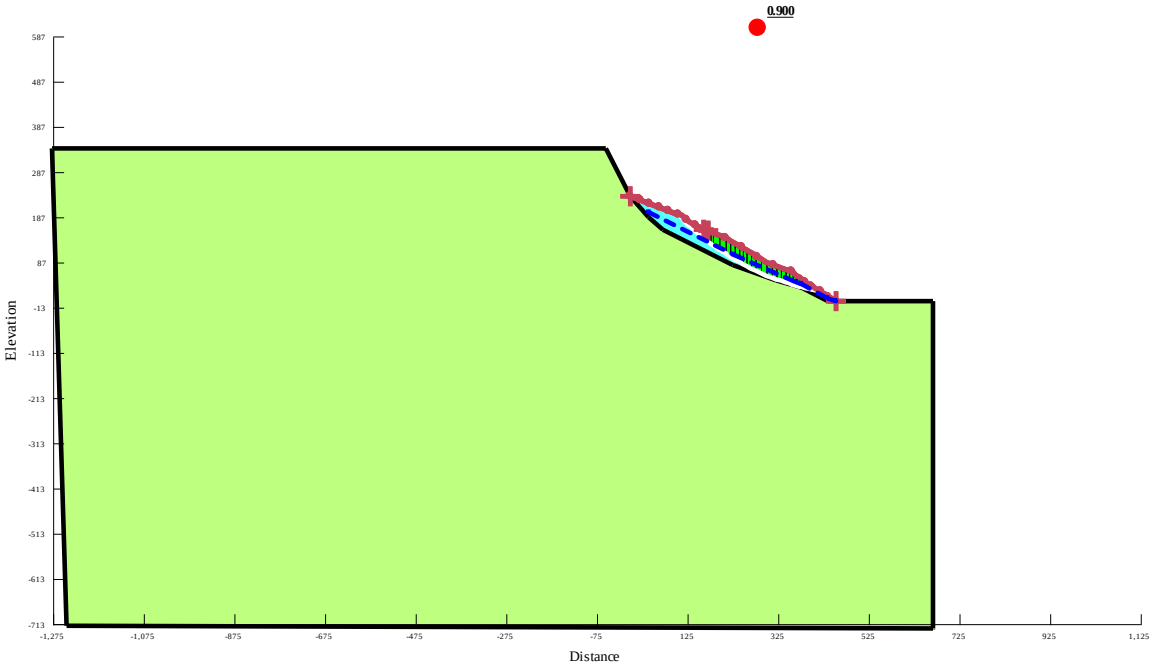

Color	Name	Model	Unit Weight (kN/m^3)	Cohesion' (kPa)	Phi' (°)	Phi-B (°)	Piezometric Line
	Rock Layer	Mohr-Coulomb	24	85	30	0	1
	Top Layer	Mohr-Coulomb	18	5	28	0	1

Figure 5. 14: Model in LEM for calculating FOS of back analyzed parameters.

After the analysis is carried out, the result is obtained in the format as shown in the Figure 5.15. The FOS value of 0.900 is obtained from the back analyzed parameters. The failure surface is shown in the figure below with the slices. The result obtained will be discussed in the next Chapter of this thesis report.

This model is again used for various trials to back calculate the mobilized parameters at the time of failure. The trails are initially carried out varying the water table surface or by probabilistic approach if required.

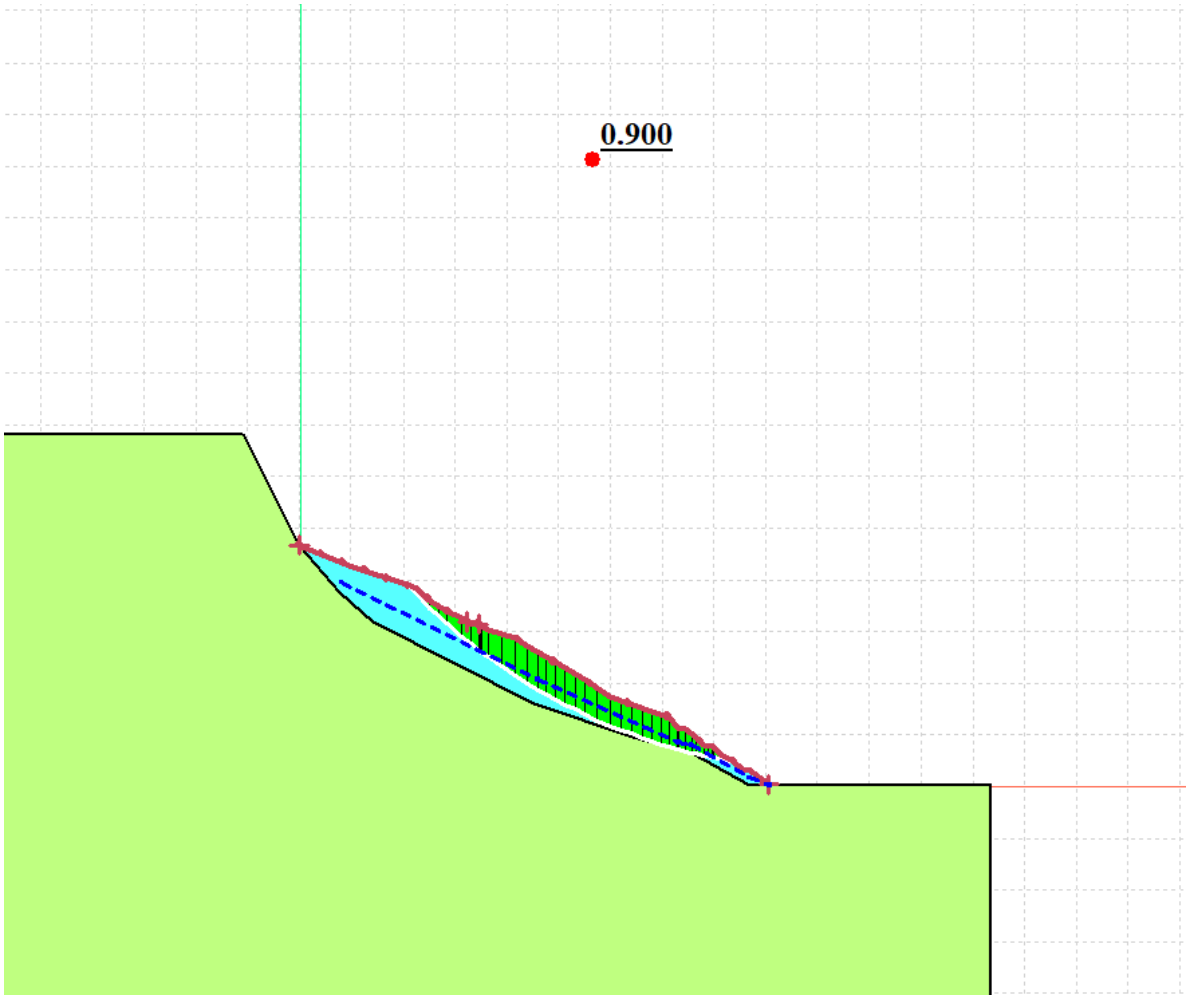

Figure 5. 15: FOS calculation at 8m water table from original water table.

5.15 FOS at 7m rise in water table

The FOS value for the 8m rise in water table using back analyzed parameters was found to be 0.900. The water table is decreased by 1m to calculate the FOS using all the parameters same as in previous model. The model is prepared and the analysis is carried out.

The FOS value of 0.922 is obtained from the back analyzed parameters which is in increasing order than water table being at 8m. The failure surface is shown in the figure below with the slices in Figure 5.16. The result obtained will be discussed in the next Chapter of this thesis report.

Figure 5. 16: FOS calculation at 7m water table from original water table.

5.16 FOS at 6m rise in water table

The FOS value for the 8m and 7m rise in water table using back analysed parameters was found to be 0.900 and 0.922. The water table is decreased by 1m to calculate the FOS using all the parameters same as in previous model. The model is prepared and the analysis is carried out.

The FOS value of 0.942 is obtained from the back analyzed parameters which is in increasing order than water table being at 8m. The failure surface is shown in the figure below with the slices in Figure 5.16. The result obtained will be discussed in the next Chapter of this thesis report.

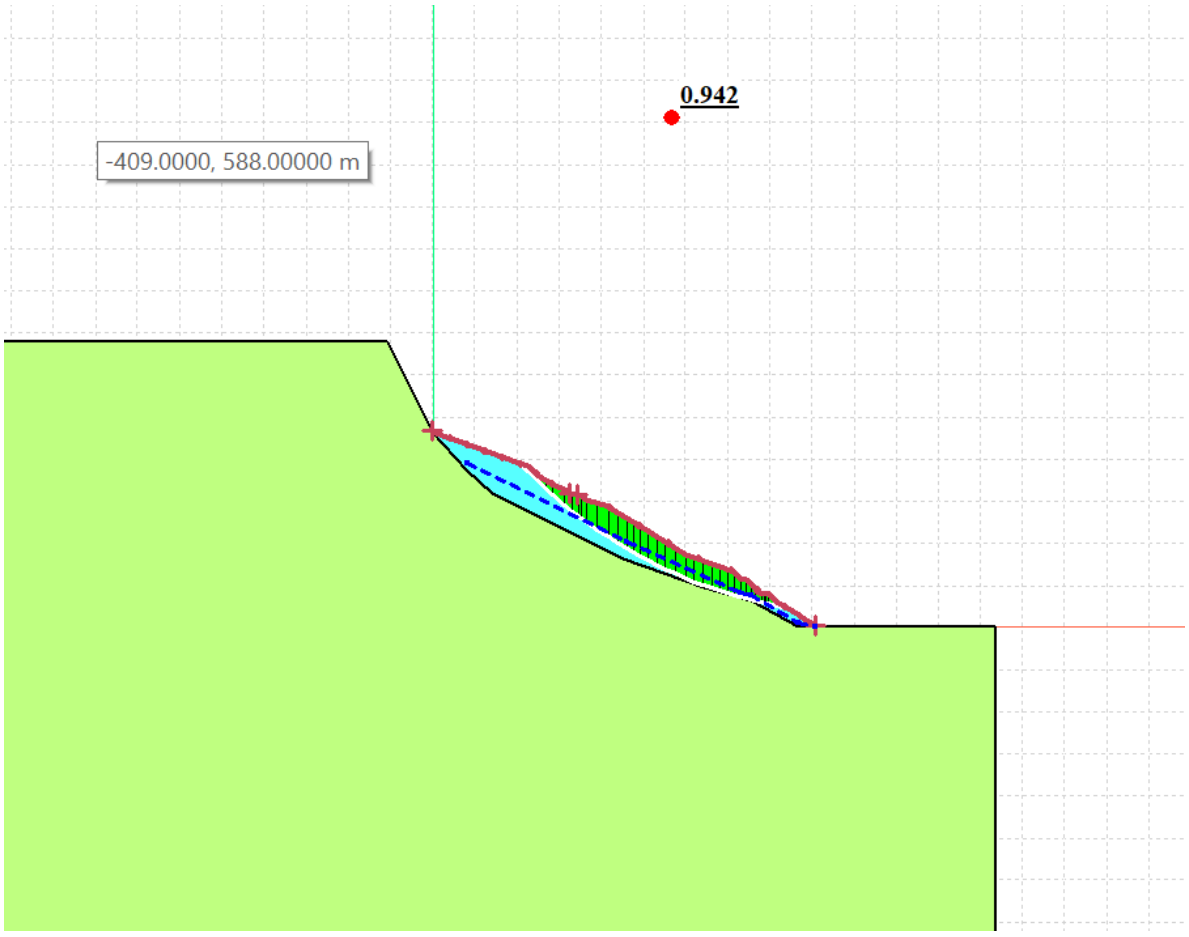

Figure 5. 17: FOS calculation at 6m water table from original water table.

5.17 FOS at 3m rise in water table

The FOS value for the 8m, 7m and 6m rise in water table using back analysed parameters was found to be 0.900, 0.922 and 0.942. The water table is decreased by 3m i.e. to the level of 3m to calculate the FOS using all the parameters same as in previous model. The model is prepared and the analysis is carried out.

The FOS value of 1.001 is obtained from the back analyzed parameters which is in increasing order than water table being at 8m. The failure surface is shown in the figure below with the slices in Figure 5.16. The Factor of Safety value is nearly equal to one in this case. The result obtained will be discussed in the next Chapter of this thesis report.

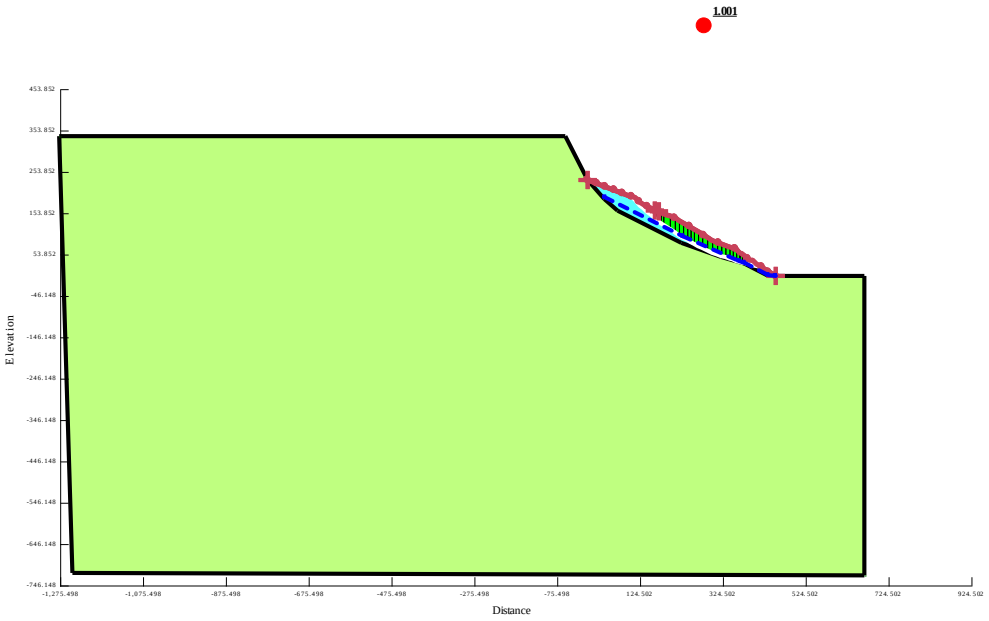

Color	Name	Model	Unit Weight (kN/m³)	Cohesion' (kPa)	Phi' (°)	Phi-B (°)	Piezometric Line
	Rock Layer	Mohr-Coulomb	24	85	30	0	1
	Top Layer	Mohr-Coulomb	18	5	28	0	1

Figure 5. 18: FOS calculation at 3m water table from original water table.

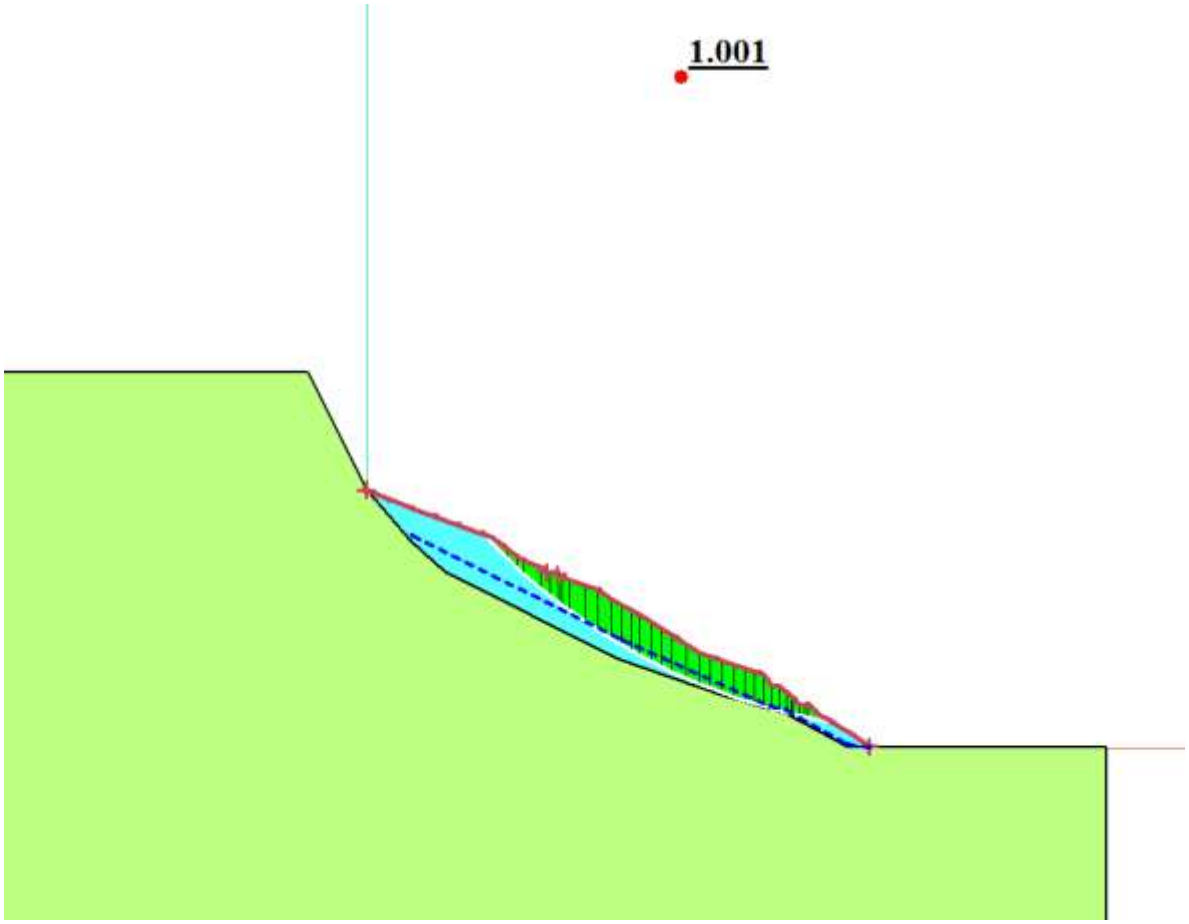

Figure 5. 19: Expanded view of FOS calculation at 3m water table from original water table.

6. Discussion

Landslide is observed at the slope in the Singati Bazar of Dolakha district. There is the settlement in the area of the slide. The debris from the slide have disturbed the buildings which are in its path. This slope instability may result huge destruction of properties, human lives and infrastructures nearby.

This study gives the clear insight of the stability analysis of the slopes failure using different methods of analysis by numerical modelling and field verifications of the specified Singati landslide.

The model using the cross section X2 as shown in Figure 3.1 were prepared which represented the section for the maximum number of Pillars (Pillar1, Pillar 2, Pillar 3, Pillar 4, Pillar 5 and Pillar 6). The models were prepared for the analysis of the slope located in Singati Bazar using the FEM and LEM approaches. The model parameters were back calculated using the field measurement deformation values using FEM. Many numbers of trials were performed varying the values of c', ϕ' and Υ. The parameters as shown in Table 6.1 were fixed using the field measured deformation data which showed the similar deformation pattern as recorded in the field in FEM analysis.

After the values of c', ϕ' and Υ were finalized which show the matching deformation pattern as obtained in field, the trials were started increasing the water table by 1m of the original water table to match the deformation obtained from the field measurement. The trials increasing the water table by 1m, 3m, 4m, 5m, 6m, 7m, 8m, 9m and 10m were carried out.

The deformation in the slope with variation in water table has been studied by various researchers in the past. The similar kind of study of deformation with the increase in water table was carried out in the Phd thesis work by Mohamed Farouk Mohamed Ibrahim Mansour. He had analyzed the deformation with variation in water table.

The results of these trials carried out increasing the water table from original water table (dry season water table) showed that the deformation increase with increase in water table. This justifies the movement of the slope in the period of Shrawan month end and first half of Bhadra month.

The result for the trial in which 8m rise in water table was considered matched the vertical displacement of Pillars: Pillar 1, Pillar2, Pillar 3, Pillar 4, Pillar6 and Pillar 7

lying around studied cross section X2 in the field. The output of the FEM model with the recorded deformation at 8m water table is presented in Table 6.1.

Table 6. 1: Model parameters obtained from back analysis in FEM.

Material	Unit Weight (kN/m^3)	Friction Angle(deg)	Cohesion(kPa)
Top Layer	18	28	5
Rock Layer	24	30	85

The borehole log shows the top layer consisting of medium to coarse grained sand with flakes of schist and cobble of slightly weathered schist and the rock layer consisting of bedrock of fine grain, slightly weathered schist with quartz veins.

The parameters fixed from FEM analysis as presented in Table 6.1 are again used in LEM to carry out the Factor of Safety Values. It is done to analyze the Factor of safety of the slope with the variation in water table and what stage we obtain the FOS value of 1 where the slope will fail.

These model parameters obtained from FEM were again modelled in LEM to calculate the Factor of Safety of the modelled slope. The results presented in Table 6.1 was used in LEM model to calculate the Factor of Safety Value. The FOS value of 0.900 was obtained. The trial were further carried out reducing the water table in LEM to obtain the FOS value of 1 which represent the slope at failure. Then the mobilized parameters are used for analyzing the mitigating measures of the slope instability. The output of different trials in LEM to calculated Factor of Safety are as shown in Table 6.2.

Table 6. 2: Factor of Safety values obtained from LEM for variation in water table.

S.N	Water table rise by	Factor of Safety
1	8m	0.900
2	7m	0.922
3	6m	0.942
4	3m	1.001

The results obtained showed that the major causes of the slope failure to be increase in the ground water table which is due to the precipitation and ground water recharge flowing through the cultivable land to the slope without any drainage arrangements. These arguments were supported by the field verifications as the landslide was mostly in between the end of Shrawan month and middle of Bhadra month in recent years. The results from the field measurement and the results from FEM also showed the maximum deformation in that period.

The mitigation model for the slope was prepared by carrying out the trails by further decreasing the water table and checking the Factor of Safety of the slope. After decreasing the water table to the original ground water table measured in Magh month, Factor of Safety value of 1.05 is achieved which is presented in the Figure 6.1.

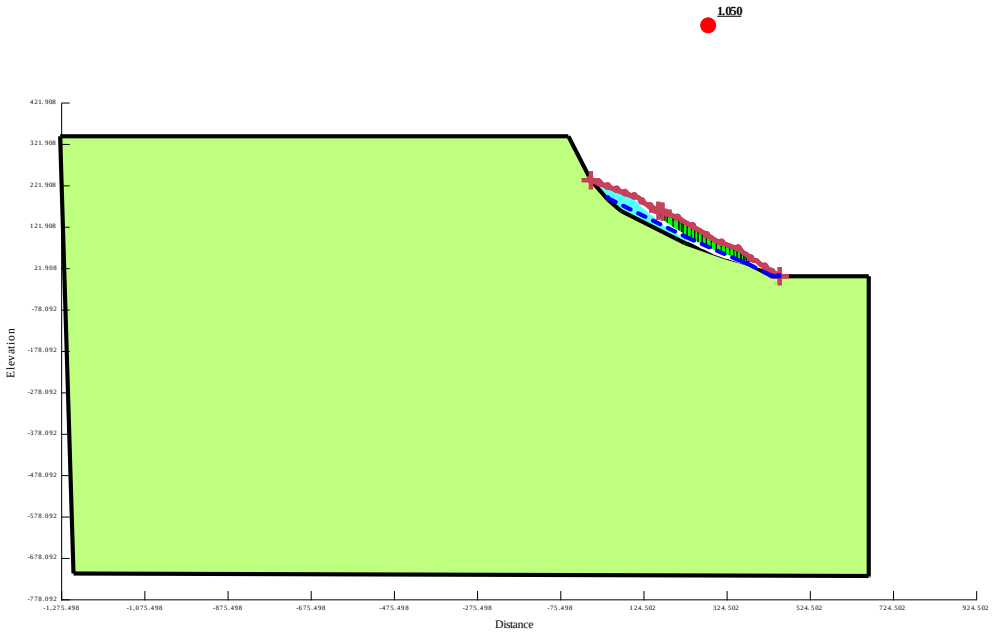

Color	Name	Model	Unit Weight (kN/m³)	Cohesion' (kPa)	Phi' (°)	Phi-B (°)	Piezometric Line
	Rock Layer	Mohr-Coulomb	24	85	30	0	1
	Top Layer	Mohr-Coulomb	18	5	28	0	1

Figure 6. 1: FOS calculation at original water table.

With the decrease in water table in the slope, the internal friction angle of the material increases. The model is prepared considering the increase in internal friction angle to increase up to 33°. The increased ϕ value is taken as the average in the overall top layer and Factor of Safety of 1.276 is obtained as shown in Figure 6.2.

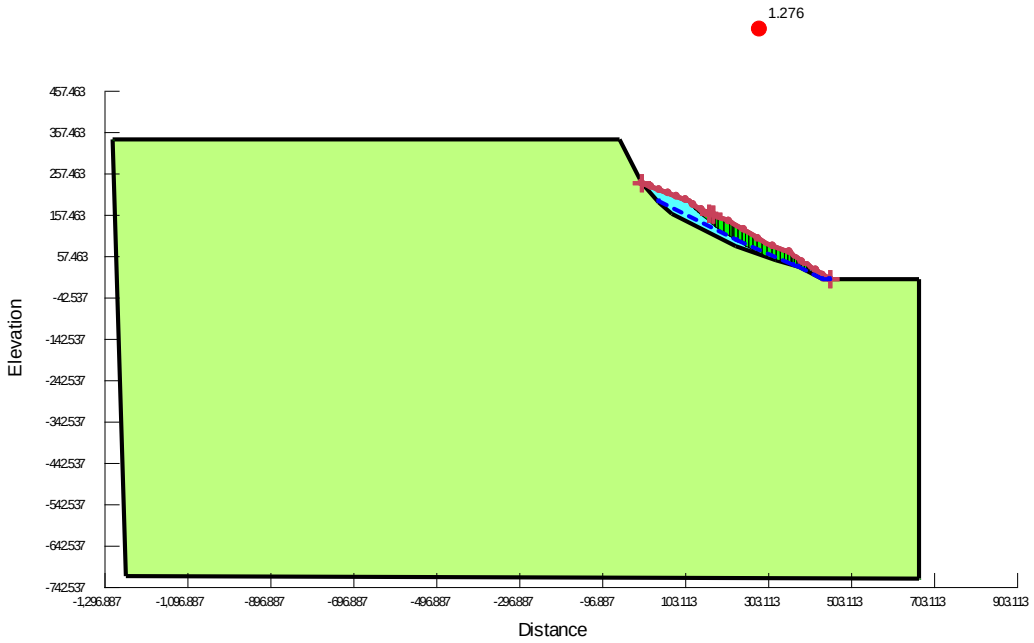

Color	Name	Model	Unit Weight (kN/m³)	Cohesion' (kPa)	Phi' (°)	Phi-B (°)	Piezometric Line
	Rock Layer	Mohr-Coulomb	24	85	30	0	1
	Top Layer	Mohr-Coulomb	18	5	33	0	1

Figure 6. 2: FOS calculation after strength regain consideration.

After the decrease in water table showed the increased stability of the slope, the basic recommendation for mitigation measures such as surface and subsurface drainage, protection walls in the road sides and soil nailing in the toe area of the slope are recommended as shown in the Figure 6.3 which shall be verified and designed by the experts.

Figure 6. 3: Recommended Protection measures.

7. Conclusion

Landslide is observed at the slope in the Singati Bazar of Dolakha district. There is the settlement in the area of the slide. The debris from the slide have disturbed the buildings which are in its path. The infrastructures like road, bridge over Singati River are subjected to risk. This slope instability may result huge destruction of properties, human lives and infrastructures nearby.

The study of the nature, amount and cause of deformation was essential for the understanding of the slope failure. The specific objective of this study was to analyze the slope stability of the study area from the Numerical Modelling with verification from deformation measurement and to analyze the performance of mitigation measures such that it can further verify the major triggering factor of slope movement.

The literatures relating to finding the causes of slope failure, slope movements, are referred. The literatures are referred for analyzing the performance of mitigation measures such as to further verify the major triggering factor of Slope movement. He had analyzed the slope movement with variation in water table.

The slope stability analysis of the Singati slope is analyzed by methodology developed for this thesis. The back analysis of the slope was performed using the field measurement of the deformation and the model parameters were determined using FEM. The model parameters determined were again used to calculate the FOS of the slope using LEM.

The results in FEM showed the increase in vertical displacement values with the increase in water table with relative to dry weather water table. The results using LEM showed that the increase in the FOS value with the decrease in water table. The model with the same parameters and ground water table at 8m, 7m, 6m and 5.5m from the original ground water table gave the FOS values of 0.963, 0.974, 0.994 and 1.001. For the mitigation model, the water table was considered as the original water table or dry weather water table and all parameters obtained from FEM being same the FOS value of 1.05 is obtained.

The decreased Factor of Safety values with the increase in water table from the original water table or dry weather water table and after the water table decrease to the dry weather water table the FOS value obtained is 1.05 which proves the major triggering

factor to be the variation in water table. With the decrease in water table in the slope, the internal friction angle of the material increases. The increased ϕ value is taken as the average in the overall top layer and Factor of Safety of 1.276 is obtained as shown in Figure 6.2. This FOS of 1.276 during the dry weather suggests the slope is stable during the dry weather period and the major triggering factor is the variation in water table.

After provision of the surface and subsurface drainage and higher efficiency of the drainage system, the water table decreased to dry weather water table and strength regain consideration resulted FOS value of 1.276 which is not still sufficient. The protection measures like the retaining structures in the road side as shown in Figure 6.2, soil nailing up to the depth of 15m are recommended in the toe area of the slide zone to increase the value of strength parameters which shall further be verified by the experts.

8. References

1. Duncan, J.M. and Stark, T.D. (1992), Soil Strengths from back analysis of slope failures, Proc. Of Speciality Conf. Stability and Performance of Slopes and Embankments-II, ASCE, Berkeley, CA, June, Vol. 1, pp. 890-904.
2. Handwerger, A. L., Huang, M.-H., Fielding, E. J.,Booth, A. M. & Bürgmann, R. A shift from drought to extreme rainfall drives a stable landslide to catastrophic failure. *Sci. Rep.* 9, 1569 (2019).
3. Jagriti Mandal, Sruti Narwal, and S.S. Gupte, Back Analysis of a Failed Slopes – A Case Study, Intenational Journal of Engineering Research & Technology, Vol.6 Issue 05, May-2017.
4. J.Zhang, Wilson H. Teng and L.M.Zang (2010), Efficient Probabilistic Back Analysis of Slope Stabilty Model Parameters, Journal of Geotechnical and Geoenvironment Engineering, Vol136, No. 1, Jan 2010, PP 99-109.
5. Leroueil, S., Locat, J., Vaunat, J., Picarelli, L., Lee, H., Faure, R., 1996.Geotechnical characterization of slope movements. In: Senneset (Ed.), Landslides, Proceedings of the VIIth International Symposium on Landslides, vol. 1. Balkema, Rotterdam, pp. 53–74.
6. L.L. Zhang a, J. Zhang , L.M. Zhang d, W.H. Tang d, Back analysis of slope failure with Markov chain Monte Carlo simulation,2010
7. Mohamed Mansour, Phd. Thesis on Characteristic Behavior of Slow Moving Slides.
8. Morgenstern NR, Price VE. The analysis of the stability of general slip surfaces. Geotechnique 1965; 15(1):79–93.
9. Paolo Ruggeri , Viviene M. E. Fruzzetti , Antonio Ferretti and Giuseppe Scarpelli, Seismic and Rainfall Induced Displacements of an Existing Landslide: Findings from the Continuous Monitoring,2020
10. SRokosz Piotr (2008). A paper on Back Analysis in Geotechnics - Examples of shape Determination.
11. Wilson H. Tang, Timothy D. Stark and Mauricio Angulo, Reliability in back analysis of slope failures, Japanese Geotechnical Society, Soil and Foundations Vol.39, No.5, 73-80, Oct-1999.
12. Zhang J, Tang WH, Zhang LM. Efficient probabilistic back-analysis of slope stability model parameters. J Geotech Geo environ Eng 2010; 136(1):99–109.
13. Zhang LL, Zhang J, Zhang LM, Tang WH. Back analysis of slope failure with Markov chain Monte Carlo simulation. Comput Geotech 2010; 37(7–8):905–12.